BRAIN
ORIGINAL ARTICLE

Broad activation of the Parkin pathway induces synaptic mitochondrial deficits in early tauopathy

Yu Young Jeong,[1] Sinsuk Han,[1,†] Nuo Jia,[1,†] Mingyang Zhang,[1,‡] Preethi Sheshadri,[1] Prasad Tammineni,[1,§] Jasmine Cheung,[1] Marialaina Nissenbaum,[2] Sindhuja S. Baskar,[1] Kelvin Kwan,[1] David J. Margolis,[1] Peng Jiang,[1] Alexander W. Kusnecov[2] and Qian Cai[1]

[†]These authors contributed equally to this work.

Mitochondrial defects are a hallmark of early pathophysiology in Alzheimer's disease, with pathologically phosphorylated tau reported to induce mitochondrial toxicity. Mitophagy constitutes a key pathway in mitochondrial quality control by which damaged mitochondria are targeted for autophagy. However, few details are known regarding the intersection of mitophagy and pathologies in tauopathy.

Here, by applying biochemical and cell biological approaches including time-lapse confocal imaging in live tauopathy neurons, combined with gene rescue experiments via stereotactic injections of adeno-associated virus particles into tauopathy mouse brains, electrophysiological recordings and behavioural tests, we demonstrate for the first time that mitochondrial distribution deficits at presynaptic terminals are an early pathological feature in tauopathy brains. Furthermore, Parkin-mediated mitophagy is extensively activated in tauopathy neurons, which accelerates mitochondrial Rho GTPase 1 (Miro1) turnover and consequently halts Miro1-mediated mitochondrial anterograde movement towards synaptic terminals. As a result, mitochondrial supply at tauopathy synapses is disrupted, impairing synaptic function. Strikingly, increasing Miro1 levels restores the synaptic mitochondrial population by enhancing mitochondrial anterograde movement and thus reverses tauopathy-associated synaptic failure. In tauopathy mouse brains, overexpression of Miro1 markedly elevates synaptic distribution of mitochondria and protects against synaptic damage and neurodegeneration, thereby counteracting impairments in learning and memory as well as synaptic plasticity.

Taken together, our study reveals that activation of the Parkin pathway triggers an unexpected effect—depletion of mitochondria from synaptic terminals, a characteristic feature of early tauopathy. We further provide new mechanistic insights into how parkin activation-enhanced Miro1 degradation and impaired mitochondrial anterograde transport drive tauopathy-linked synaptic pathogenesis and establish a foundation for future investigations into new therapeutic strategies to prevent synaptic deterioration in Alzheimer's disease and other tauopathies.

1 Division of Life Science, Department of Cell Biology and Neuroscience, School of Arts and Sciences, Rutgers, The State University of New Jersey, Piscataway, NJ 08854, USA
2 Department of Psychology, School of Arts and Sciences, Rutgers, The State University of New Jersey, Piscataway, NJ 08854, USA

[‡]Present address: Institute of Forensic Medicine, Soochow University, 178 Ganjiang East Road, Suzhou, Jiangsu 215021, China
[§]Present address: Department of Animal Biology, School of Life Sciences, University of Hyderabad, Hyderabad, Telangana 500046, India

Received January 26, 2021. Revised May 20, 2021. Accepted June 17, 2021. Advance access publication January 12, 2022

Correspondence to: Qian Cai, MD, PhD
Division of Life Science, Department of Cell Biology and Neuroscience
School of Arts and Sciences, Rutgers, The State University of New Jersey
604 Allison Road, Piscataway, NJ 08854, USA
E-mail: cai@biology.rutgers.edu

Keywords: Alzheimer's disease; mitochondrial anterograde transport; Parkin-mediated mitophagy; synaptic mitochondrial deficits; tauopathy

Abbreviations: AAV = adeno-associated virus; CCCP = carbonyl cyanide *m*-chlorophenylhydrazone; FTD = frontotemporal dementia; mEPSCs = miniature excitatory postsynaptic currents; Miro1 = mitochondrial Rho GTPase 1; OCR = oxygen consumption rate; phospho-tau = hyperphosphorylated tau; TEM = transmission electron microscopy; TMRE = tetramethylrhodamine ethyl ester

Introduction

Mitochondria are cellular energy power plants that supply ATP to fuel various activities essential for neuronal function and survival. Mitochondrial dysfunction in the nervous system is a central concern during ageing and has been associated with major incapacitating neurodegenerative disorders, including Alzheimer's disease. Mitochondrial defects are a prominent feature of both familial and sporadic Alzheimer's disease and play an important role in the early pathophysiology of Alzheimer's disease.[1–3] Pathogenic hallmark features in Alzheimer's disease brains are the presence of extracellular amyloid plaques consisting of amyloid-β and intracellular neurofibrillary tangles composed of hyperphosphorylated tau (phospho-tau), encoded by the *MAPT* gene. Of note, strong evidence supports a direct role of phospho-tau and neurofibrillary tangles in the pathogenesis of Alzheimer's disease and other neurodegenerative diseases.[4,5] Clinically, tau pathology correlates with dementia better than amyloid plaques.[6] Mutations in the *MAPT* gene are causal for a subtype of frontotemporal dementia (FTD). Experimentally, overexpression of FTD-associated *MAPT* mutant genes in transgenic mice results in neurofibrillary tangle development and neurodegeneration,[6–8] establishing the neurotoxicity conferred by the mutant tau proteins. Therefore, understanding the mechanisms underlying phospho-tau-mediated neurotoxicity is thus of great importance in developing tau-based therapy for treating diseases of tauopathy, including Alzheimer's disease.

Aberrant accumulation of phospho-tau causes mitochondrial damage by specifically impairing complex I activity of the mitochondrial respiratory chain. This leads to increased levels of reactive oxygen species, lipid peroxidation, decreased activities of detoxifying enzymes such as superoxide dismutase and mitochondrial membrane potential ($\Delta\psi_m$) dissipation.[9–13] Phospho-tau interacts with the voltage-dependent anion channel 1 (VDAC1), blocking mitochondrial pores and thus impairing mitochondrial function.[14] Pathogenic forms of tau have also been reported to interfere with mitochondrial dynamics and transport.[9,12,13,15,16] On the other hand, in tauopathy brains, altered mitochondrial function and increased reactive oxygen species production were reported to precede neurofibrillary tangle pathology and contribute to neurodegeneration.[17–19]

Aged and dysfunctional mitochondria are not only less effective in energy production and Ca^{2+} buffering, but also release harmful reactive oxygen species, compromising support of synaptic function. Mitophagy, a cargo-selective autophagy for removal of damaged mitochondria, constitutes a key cellular mechanism of mitochondrial quality control involving sequestration of damaged mitochondria within autophagosomes for lysosomal degradation.[16,20,21] Mitophagy is the only known cellular pathway through which entire mitochondria are eliminated within lysosomes, with PINK1/Parkin-mediated mitophagy being the most heavily studied and the best-understood pathway.[16,20–23] We and others have revealed that Parkin-mediated mitophagy predominantly occurs in the soma of neurons, where mature lysosomes are mainly located.[24–27] Upon mitophagy induction, anterograde transport of mitochondria in axons is significantly reduced. This is attributed to Parkin activation-enhanced proteasomal degradation of mitochondrial Rho GTPase (Miro1, encoded by *RHOT1*), a component of the adaptor–motor complex essential for KIF5 motors to drive mitochondrial anterograde movement.[28–32] Some unique features of mitophagy in normal neurons have been described. However, mechanistic understanding of neuronal mitophagy and its link to pathological conditions is still limited.

The mitochondrial quality control mechanism underlying mitochondrial defects in Alzheimer's disease remains poorly understood.[12,13,16] Even though autophagocytosis of mitochondria in the neuronal soma was reported to be a prominent feature in Alzheimer's disease patient brains,[33,34] mitophagy abnormalities in Alzheimer's disease, particularly in the PINK1/Parkin pathway, have been demonstrated in several recent studies.[35–40] For instance, Alzheimer's disease brains displayed reduced PINK1 levels while overexpression of PINK1 was shown to abolish Alzheimer's disease pathology and ameliorate cognitive dysfunction in Alzheimer's disease models.[36–38,40] Our previous studies have revealed that Parkin-mediated mitophagy is activated in the brains of Alzheimer's disease patients and mutant human amyloid precursor protein transgenic mouse models.[35] However, the mechanisms underlying mitophagy regulation under phospho-tau-associated conditions have been understudied, and few details are known regarding the intersection of mitophagy and pathologies in tauopathy.

In the current study we reveal, for the first time, that deficits in the synaptic distribution of mitochondria and extensive induction of Parkin-mediated mitophagy are early features in tauopathy brains. However, broad Parkin activation in tauopathy neurons accelerates degradation of Miro1 and consequently arrests Miro1-mediated mitochondrial anterograde transport. Such a defect disrupts mitochondrial supply to tauopathy synapses and leads to synaptic failure. Excitingly, elevated Miro1 expression restores synaptic mitochondrial pools and energy supply by enhancing anterograde transport of mitochondria, thereby protecting against synaptic damage and cognitive deficits in tauopathy mice. Thus,

our work uncovers an important early mechanism by which excessive activation of the Parkin pathway drives the pathogenesis of tauopathy-linked synaptic defects. Moreover, our study provides molecular and cellular targets for potential therapeutic approaches aimed at enhancing synaptic supply of healthy mitochondria to prevent synaptic deterioration at the early stages of tauopathy diseases, including Alzheimer's disease.

Materials and methods

Mouse line and animal care

TauP301L (rTg4510) and tauP301S (PS19) transgenic mouse lines[7,41] were purchased from the Jackson Laboratory. All animal procedures were carried out following the Rutgers Institutional Animal Care and Use Committee. The animal facilities at Rutgers University are fully Association for Assessment and Accreditation of Laboratory Animal Care accredited.

Human brain specimens

Post-mortem brain specimens from Alzheimer's disease and FTD patients and age-matched control subjects were obtained from the Harvard Tissue Resource Center and the Human Brain and Spinal Fluid Resource Center at The University of California, Los Angeles. The specimens were from the frontal cortex and were quick-frozen (BA9). Seven control subjects and eight patient brains with post-mortem interval 7.25–27.8 h were used for the purification of synaptosomal and mitochondrial fractions. Detailed information for each of the cases studied is shown in Supplementary Table 2.

Adeno-associated virus design and injection

The adeno-associated virus (AAV) constructs were built using standard molecular biology techniques. All constructs were self-complementary AAV genomes with a chicken beta actin hybrid promoter and bovine growth hormone polyadenylation signal. The upstream cDNA in both constructs was mCherry with a mutated stop codon. In the control construct, a stop codon was engineered 3′ to the 2 A sequence and no second gene was inserted. The Miro1 construct contained the mouse cDNA in frame 3′ to the 2 A sequence. The AAV2/9-mCherry-Miro1 construct contains an internal ribosome entry site segment between human Miro1 and mCherry sequences, resulting in separate expression of Miro1 and mCherry. The AAV2/9-mCherry and AAV2/9-mCherry-Miro1 viruses were produced by Vector BioLabs. Adult non-transgenic and tauP301L transgenic (rTg4510) or tauP301S transgenic (PS19) mice at 2–3 months of age were injected into the hippocampus (AP: –2 mm, LAT: –1.5 mm, DV: +1.75 mm) and the cortex (anterior-posterior: +1.5 mm, lateral: +1.5 mm, dorsal-ventral: +1.5 mm) of both cerebral hemispheres according to the stereotaxic atlas of Franklin and Paxinos[42] using 4–8 $\times$ 10^9 total viral particles per side and analysed 6–8 months after injection (Supplementary Fig. 8A).

Behaviour tests and electrophysiological studies

We performed behavioural studies to examine non-spatial and spatial learning and memory along with synaptic plasticity as previously described[43–45] (Supplementary material).

Statistical analysis

All data are presented as the mean ± standard error of the mean (SEM). All statistical analyses were performed using Prism 9 (GraphPad Software) and Minitab 19. Statistical significance was assessed by a paired *t*-test (for two group comparisons), while a two-way ANOVA test with Fisher's *post hoc* comparisons was used for multiple comparisons. *P*-values $\leqslant 0.05$ were considered statistically significant: $^{*}P < 0.05$; $^{**}P < 0.01$; $^{***}P < 0.001$.

Data availability

The authors confirm that the data supporting the findings of this study are available within the article and its Supplementary material.

Results

Early deficits in the presynaptic distribution of mitochondria in tauopathy brains

Synaptic defects have been indicated in early tauopathy.[46] However, it remains largely unknown whether mitochondrial perturbation is involved in tauopathy-associated synaptic damage. Previous studies revealed a reduction in the number of axonal mitochondria in patient brains with tauopathies and mouse models.[19,47] Thus, we first determined whether tauopathy brains exhibit distribution deficits in synaptic mitochondria by examining synapse-enriched synaptosomal fractions purified from the brains of tauopathy patients and mouse models. While phospho-tau is concentrated in synaptosomal fractions from FTD patient brains (Fig. 1A), we found a pronounced reduction in mitochondrial distribution at tauopathy synapses as reflected by decreased mitochondrial protein levels relative to those in the brains of normal control subjects (Fig. 1A and B). Moreover, in Alzheimer's disease patient brains with tauopathies, synaptic terminals enriched with phospho-tau also exhibit a deficit in mitochondrial distribution compared to those of control subjects (Supplementary Fig. 1A and B). There is no detectable change in the levels of synaptophysin (SYP), a synaptic vesicle protein. Our data suggest that mitochondrial content is reduced at synaptic terminals in tauopathy brains. We further assessed a well-characterized regulatable tauopathy mouse model, rTg4510. This model overexpresses 13 units of human mutant (P301L) tau downstream of a tetracycline-operon-responsive element.[7,48] In agreement with the results from patient brains with tauopathies, the levels of mitochondrial proteins, but not synaptic proteins, are remarkably decreased in synaptosomal fractions isolated from the hippocampi of tauopathy mouse brains (Fig. 1C and D). These findings collectively indicate that deficits in the synaptic distribution of mitochondria are a marked feature in tauopathy brains.

Next, we sought to address whether such synaptic mitochondrial deficits are an early defect in tauopathy prior to axon loss and neurodegeneration. In tauP301L transgenic mouse brains at 4 months of age, before the disease onset, we performed co-immunostaining with antibodies against SYP and cytochrome c, a mitochondrial intermembrane space protein. Compared to non-transgenic littermate controls, mitochondrial density in the axon-enriched areas is significantly decreased with no change in the neuronal soma of the hippocampal CA1 regions of tauP301L transgenic mouse brains (Fig. 1E and F). Consistently, presynaptic distribution of mitochondria is dramatically reduced, while the density of presynaptic terminals in the same areas remains unaltered (Fig. 1E and G), suggesting distribution deficits in synaptic mitochondria, an early defect prior to synapse loss in tauP301L transgenic mouse brains at this age. To further confirm such a defect in association with early tauopathy, we examined a second tauopathy mouse model (PS19), which expresses human mutant (P301S) tau under the mouse prion promoter (MoPrP) to achieve 5-fold higher expression than endogenous mouse tau.[41] By conducting transmission electron microscopy (TEM) analysis, we investigated

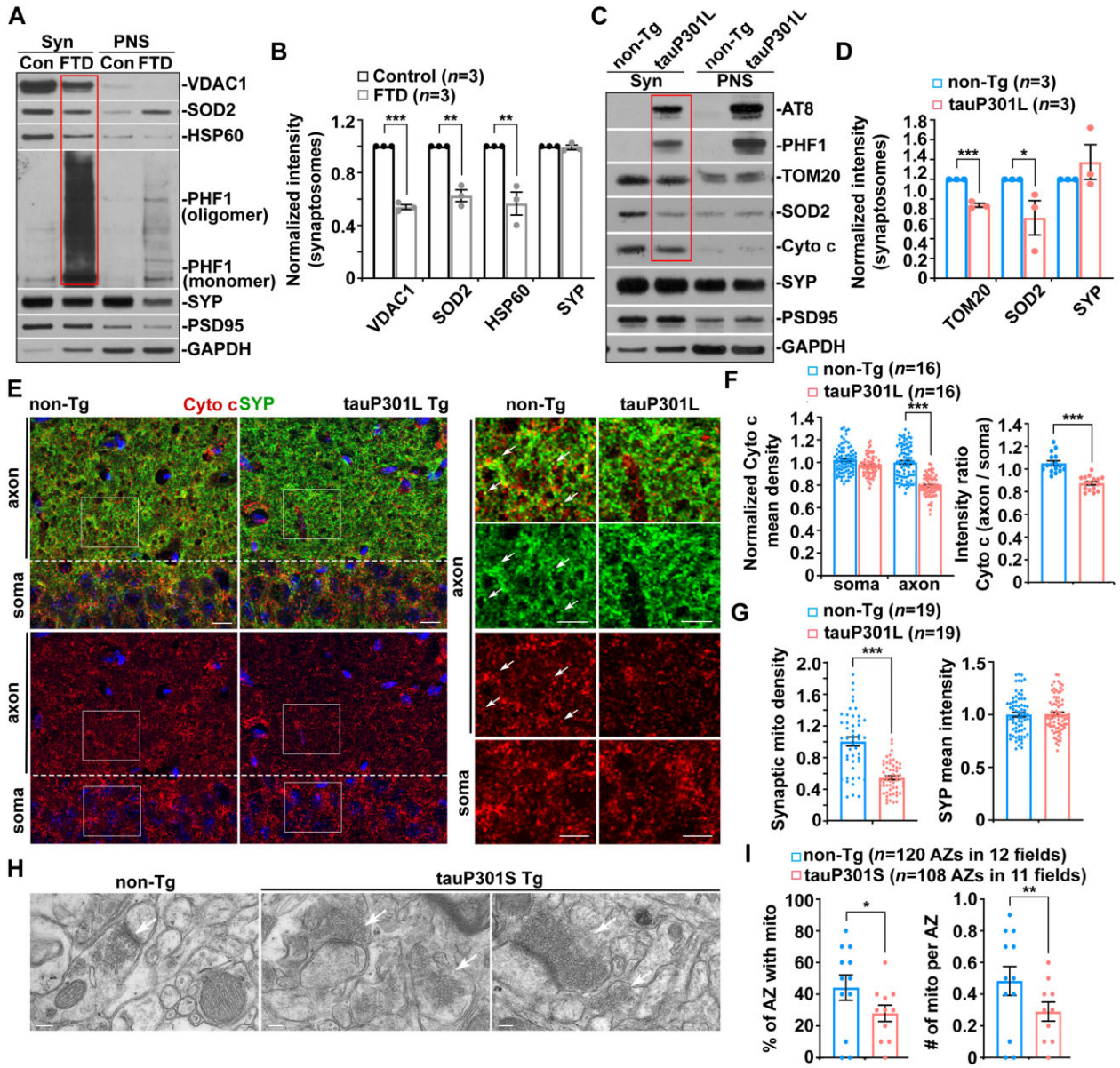

Figure 1 Early deficits in the presynaptic distribution of mitochondria in tauopathy brains. (**A** and **B**) Representative blots (**A**) and quantitative analysis (**B**) showing that mitochondrial distribution is markedly reduced at synaptic terminals enriched with phospho-tau in FTD patient brains. Equal amounts (10 μg) of synapse-enriched synaptosomal preparations (Syn) and post-nuclear supernatants (PNS) from the brains of normal control subjects and FTD patients were sequentially immunoblotted on the same membrane after stripping between each antibody application. The purity of synaptosomal fractions was confirmed by the relative enrichment of synaptic protein markers synaptophysin (SYP) and PSD95 and by less abundance of GAPDH, compared to those in post-nuclear supernatants. The intensities of proteins in the synaptosomal fractions of FTD patient brains were normalized to those in control subjects. Data were quantified from three independent experiments. (**C** and **D**) Reduction in mitochondrial content in Syn fractions purified from tauP301L transgenic (Tg) mouse brains. The protein intensities in Syn fractions from tauopathy mouse brains were normalized to those in non-transgenic (non-Tg) littermate controls. Data were quantified from three independent repeats. (**E**–**G**) Representative images (**E**) and quantitative analysis (**F** and **G**) showing a significant decrease in mitochondrial density at the SYP-marked presynaptic terminals of the hippocampal CA1 regions in tauP301L transgenic mouse brains at the age of 4 months. There is no detectable change in mitochondrial distribution in the soma of hippocampal neurons along with the density of presynaptic terminals. Data were expressed as the mean intensities of SYP or cytochrome *c* (Cyto c), the intensity ratio of cytochrome *c* between axon and soma, or mitochondrial density at presynaptic terminals per imaging hippocampal slice section (320 × 320 μm), which were normalized to those from non-transgenic littermate controls. Data were quantified from a total number of slice sections indicated in parentheses (**F** and **G**). (**H** and **I**) Representative transmission electron microscopy (TEM) images (**H**) and quantitative analysis (**I**) showing a decrease in the number of mitochondria at presynaptic terminals, indicated by white arrows, in the hippocampal regions of 5-month-old tauP301S transgenic mouse brains. The percentage of the active zone (AZ) containing mitochondria and the number of mitochondria per active zone in tauP301S mouse brains were quantified and compared to those in non-transgenic littermate controls. Data were quantified from the total numbers of active zones and imaging fields indicated in parentheses (**I**). Scale bars = 10 μm (**E**); and 200 nm (**H**). Error bars represent SEM. Student's *t*-test: ***$P < 0.001$; **$P < 0.01$; *$P < 0.05$.

the presynaptic distribution of mitochondria at the ultrastructural level in the hippocampi of 5-month-old tauP301S transgenic mouse brains at early disease stages. TauP301S mice display drastic decreases in the percentage of active zone containing mitochondria and the number of mitochondria per active zone in the hippocampal synapses, relative to those of non-transgenic controls (Fig. 1H and I). Moreover, we detected mitochondrial reduction in the axon-enriched regions, but not in the soma of hippocampal areas of tauP301S transgenic mouse brains (Supplementary Fig. 1C and E), coupled with decreased mitochondrial distribution at presynaptic terminals (Supplementary Fig. 1D and E). The densities of presynaptic terminals and neurofilament-labelled axons in the same areas of this tauopathy mouse model did not exhibit detectable alterations at this stage (Supplementary Fig. 1D and E–G). Also, we did not observe a significant reduction in axons stained by neurofilament antibody in 4-month-old tauP301L transgenic mouse brains (data not shown). These observations from confocal imaging study and TEM analysis in these two different tauopathy mouse models are consistent with biochemical evidence from tauopathy brains, suggesting that distribution deficits of presynaptic mitochondria are linked to early tauopathy prior to the loss of synapses and axons.

Impeded mitochondrial anterograde transport coupled with mitochondrial stress in early tauopathy

Anterograde transport delivers newly generated healthy mitochondria from the soma towards axonal terminals, playing a major role in the control of mitochondrial supply and distribution at presynaptic terminals. This maintains energy homeostasis and powers synaptic transmission.[15,21] Therefore, we next determined whether mitochondrial distribution deficits at tauopathy synapses are caused by impaired anterograde transport that fails to supply mitochondria to distal axon areas. We examined mitochondrial movement by conducting time-lapse imaging in live primary cortical neurons cultured from tauP301S transgenic mouse brains. Neurons were transfected with DsRed-Mito, followed by imaging at 9–10 days *in vitro* (DIV). We have found that mitochondrial anterograde transport is impaired in tauP301S axons in comparison with that of control axons from non-transgenic littermates (Fig. 2A and B). As an internal control, retrograde transport of mitochondria along the same axons does not show any change, thus excluding the possibility of microtubule destabilization or disassembly in tauP301S axons. Moreover, the number of mitochondria is decreased within the same axons (Fig. 2A and B), suggesting that defective anterograde transport disrupts mitochondrial supply to tauopathy axons. We further assessed whether such a defect is related to phospho-tau accumulation. In line with the results from tauP301S transgenic neurons (Fig. 2A and B), axons expressing tauP301L, but not tau or vector controls, display decreased mitochondrial anterograde movement, whereas retrograde transport is not affected along the same axons. TauP301L-expressed axons also exhibited a reduced number of mitochondria (Supplementary Fig. 2A and B). Our data suggest that impaired mitochondrial anterograde transport is a defect related to the burden of phospho-tau, disrupting the supply of mitochondria to distal tauopathy axons.

By performing multiple lines of experiments, we next assessed whether other mitochondrial alterations are linked to early tauopathy conditions. First, we measured $\Delta\psi_m$ in non-transgenic and tauP301S transgenic neurons. Tetramethylrhodamine ethyl ester (TMRE), a $\Delta\psi_m$-dependent dye, was loaded into live neurons expressing mitochondrial marker CFP-Mito. Healthy mitochondria accumulate TMRE, thus displaying high TMRE intensity,[24,27,35] whereas damaged mitochondria with depolarized $\Delta\psi_m$ show reduced TMRE fluorescent intensity, although they retain CFP-Mito signals. In non-transgenic neurons, the majority of CFP-Mito–labelled mitochondria were co-labelled by TMRE, reflecting their electrochemically active status (Fig. 2D). In contrast, somatic mitochondria in tauP301S transgenic neurons display reduced TMRE fluorescence, suggesting depolarized $\Delta\psi_m$ (Fig. 2C and D). TMRE mean intensity in tauP301S neurons is significantly reduced relative to that of non-transgenic littermate controls (Fig. 2C). Second, we examined mitochondrial oxidative stress in the soma and the axons of tau neurons using Matrix-roGFP, RoGFP (reduction–oxidation-sensitive green fluorescent protein) in mitochondrial matrix.[49,50] Compared to non-transgenic littermate controls, tauP301S transgenic neurons exhibit a robust increase in oxidized mitochondria within the soma and the axon (Fig. 2E and F and Supplementary Fig. 2C). Aberrant accumulation of oxidatively damaged mitochondria is in accord with $\Delta\psi_m$ depolarization, suggesting enhanced mitochondrial damage in tauopathy neurons. Third, we measured cellular ATP levels to determine whether mitochondrial damage in tauP301S neurons impairs mitochondrial energetics. We utilized AT1.03, a genetically encoded Förster resonance energy transfer (FRET)-based ATP indicator,[51] in which the ε subunit of *Bacillus subtilis* F_oF_1-ATP synthase was connected to yellow (YFP) and cyan (CFP) fluoresent protein. Given that the ATP-bound form increases FRET efficiency, enhanced FRET signal (YFP/CFP emission ratio) indicates an increase in cellular ATP levels. TauP301S neurons show lower YFP/CFP ratios in both the soma and the axons of neurons than those in non-transgenic littermate control neurons (Fig. 2G and H), indicating reduced mitochondrial energetic activity in tauopathy neurons. To confirm these *in vitro* observations, we further examined the oxygen consumption rate (OCR) in mitochondria freshly isolated from the cortices of non-transgenic or tauP301L transgenic mouse brains at 3–4 months of age. Compared to non-transgenic controls, basal and maximal respiration rates along with ATP production-linked respiration in mitochondria are significantly decreased in tauP301L mouse brains (Fig. 2I). This result suggests that mitochondrial oxidative phosphorylation activity is impaired in tauopathy mouse brains before the disease onset. Thus, our *in vitro* and *in vivo* findings consistently reveal that mitochondrial perturbation is associated with early tauopathy.

Broad activation of Parkin-mediated mitophagy in tauopathy brains

Mitophagy constitutes a key mitochondrial quality control system in neurons by which damaged mitochondria are sequestered within autophagosomes for lysosomal degradation to maintain mitochondrial homeostasis.[16,21] Next, we addressed whether mitophagy is induced upon mitochondrial damage in early tauopathy. We first conducted immunohistochemistry in the tauP301L transgenic mouse model at 4 months of age. In non-transgenic mouse brains, the autophagic marker LC3 appeared as a diffuse pattern predominantly present in the cytoplasm of hippocampal neurons. In tauP301L transgenic mouse brains, however, a majority of LC3 associated with vesicular structures as LC3-II-decorated autophagic vacuoles are co-labelled by mitochondrial marker cytochrome *c* (Fig. 3A and B), suggesting that mitophagy is activated in tauP301L neurons. Our confocal imaging data also revealed an increased number of mitophagosomes in the hippocampal neurons of tauP301S transgenic mouse brains (Supplementary Fig. 3A). To further evaluate mitophagy activation, we carried out TEM analysis in a second tauopathy model, tauP301S transgenic mice, at the ultrastructural level. Mitochondria exhibit abnormal morphology, characterized by a swollen round shape and perturbed or absent cristae organization in the hippocampi of 5-month-old

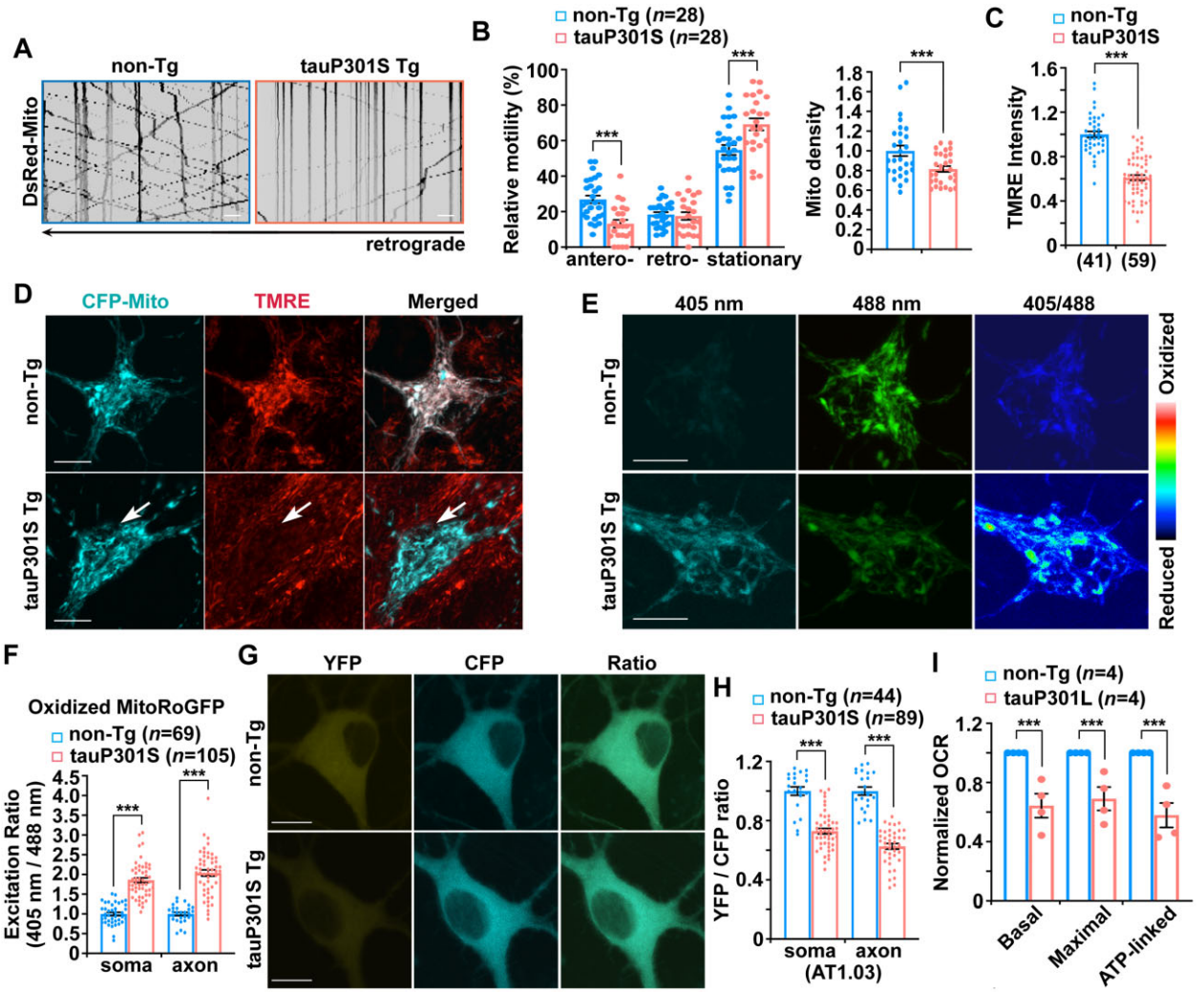

Figure 2 Impeded mitochondrial anterograde transport coupled with mitochondrial stress in early tauopathy. (**A** and **B**) Representative kymographs (**A**) and quantitative analysis (**B**) showing defects in anterograde transport, but not retrograde transport, of mitochondria along tauP301S axons. Note that defective mitochondrial anterograde transport is coupled with a reduced number of mitochondria within the same axons of cortical neurons derived from tauP301S transgenic (Tg) mouse brains. Vertical lines represent stationary organelles; slanted lines to the right (negative slope) represent anterograde movement; to the left (positive slope) indicate retrograde movement. A mitochondrion was considered stationary if it remained immotile (displacement $\leqslant 5\,\mu m$). Non-transgenic (non-Tg) or tau neurons were transfected with DsRed-Mito at DIV5, followed by time-lapse imaging at DIV8–10. (**C** and **D**) Quantitative analysis (**C**) and representative images (**D**) showing aberrant accumulation of depolarized mitochondria in the soma of tauP301S transgenic neurons. Cortical neurons cultured from non-transgenic or tauP301S transgenic mice were transfected with mitochondrial marker CFP-Mito, followed by loading with mitochondrial membrane potential ($\Delta\psi_m$)-dependent dye TMRE for 30 min prior to imaging. TMRE mean intensity was normalized to those in non-transgenic neurons. Note that tauP301S neurons display reduced TMRE mean intensity in the soma relative to that of non-transgenic neurons. (**E** and **F**) Representative images (**E**) and quantitative analysis (**F**) showing abnormal accumulation of oxidized mitochondria in the soma and the axons of tauP301S neurons. The fluorescence of MitoRoGFP was emitted at 510 nm and excited at 405 nm or 488 nm, respectively. Ratiometric images were generated from fluorescence excited by 405-nm light relative to that excited by 488-nm light. The ratio has been false coloured with the indicated heat map, with high intensity indicative of RoGFP fluorescence in a more oxidative environment. Mean fluorescence intensity ratios evoked by the two excitation wavelengths at individual mitochondria in the soma and the axon of tauP301S neurons were quantified and normalized to those of non-transgenic neurons, respectively. (**G** and **H**) Representative images (**G**) and quantitative analysis (**H**) showing that cytoplasmic ATP levels are reduced in cortical neurons derived from tauP301S transgenic mouse brains. The YFP/CFP emission ratio in the soma or the axons of tauP301S neurons expressing AT1.03 was normalized to that of control neurons from non-transgenic littermates. (**I**) Early mitochondrial defects in tauopathy mouse brains. Seahorse mitochondrial stress assay using freshly isolated cortical mitochondria from 3–4-month-old tauP301L transgenic mouse brains showing impaired mitochondrial function, as evidenced by decreases in basal, maximal and ATP production-linked respiration rates. OCR measurements of mitochondria from tauP301L transgenic mouse brains were normalized to those from non-transgenic littermate controls. Data were quantified from four independent experiments. Imaging data were quantified from a total number of neurons (n) in parentheses (**B**, **C**, **F** and **H**) from at least three independent experiments. Scale bars = 10 μm. Error bars represent SEM. Student's t-test: $^{***}P < 0.001$.

tauP301S transgenic mice at early disease stages (Fig. 3D). The percentage of abnormal mitochondria in the soma of hippocampal neurons is significantly increased in tauP301S transgenic mice when compared to non-transgenic mice (Fig. 3C and D). Strikingly, we frequently detected mitophagosomes—initial autophagic vacuole-like structures engulfing or containing abnormal mitochondria (Fig. 3D, white arrows). The average number of mitophagosomes per unit area in neuronal perikarya is remarkably increased in tauP301S transgenic mouse brains (Fig. 3C). Moreover, mitochondria in the soma of hippocampal neurons in tauP301S mouse brains display shorter mitochondrial length and smaller area (Supplementary Fig. 3B), indicating mitochondrial fragmentation. Collectively, the TEM

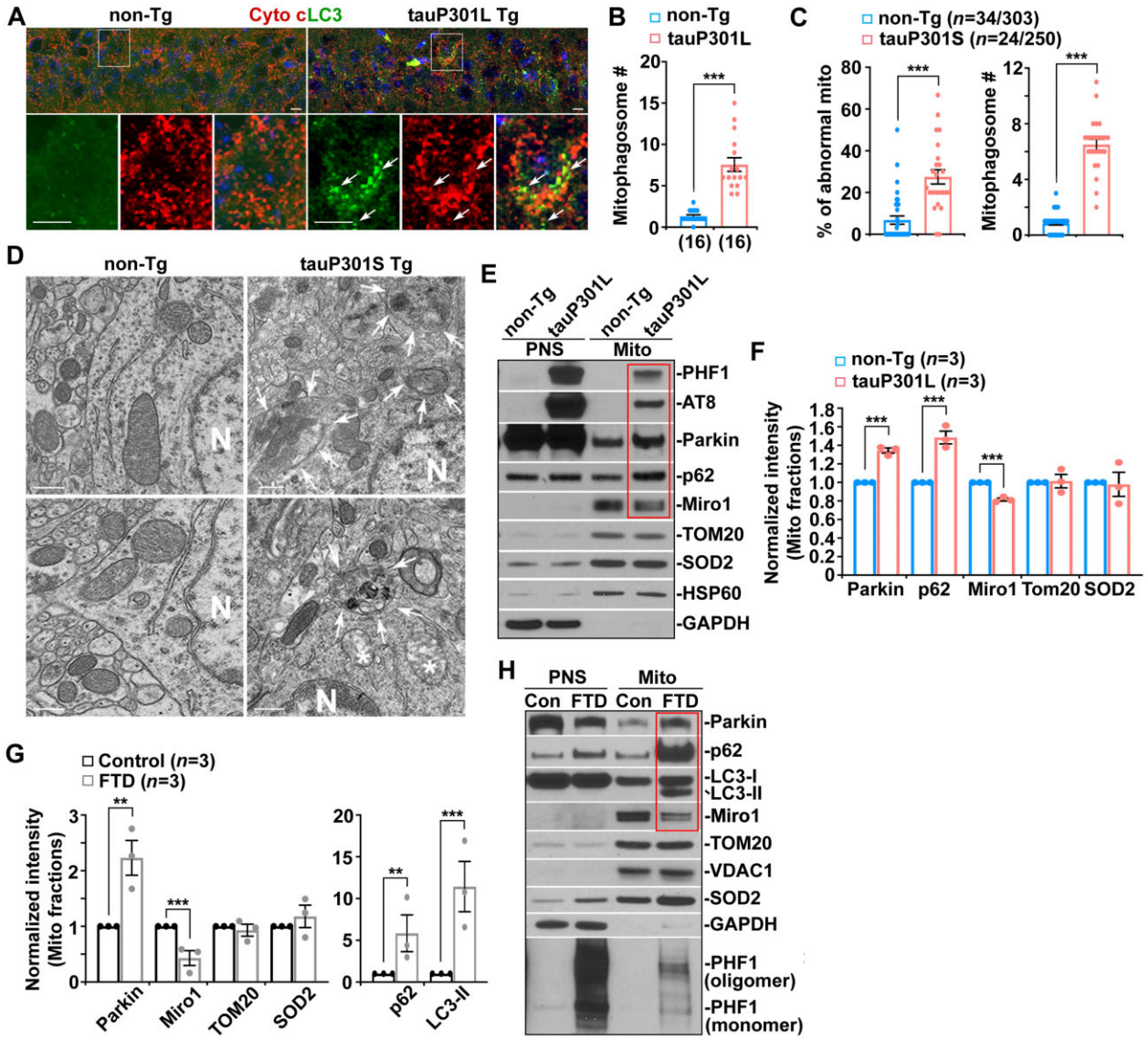

Figure 3 Broad activation of Parkin-mediated mitophagy in tauopathy brains. (**A** and **B**) Representative images (**A**) and quantitative analysis (**B**) showing an increased number of mitophagosomes in the soma of hippocampal neurons in tauP301L transgenic (Tg) mouse brains at the age of 4 months. Arrows indicate mitophagosomes co-labelled by cytochrome *c* (Cyto c) and LC3. (**B**) Data were expressed as the average number of mitophagosomes per neuronal soma per imaging hippocampal slice section (320 × 320 μm). (**C** and **D**) Quantitative analysis (**C**) and representative TEM micrographs (**D**) showing a striking accumulation of autophagic vacuoles and mitophagosome-like structures—autophagic vacuoles containing engulfed mitochondria—in the soma of hippocampal neurons in 5-month-old tauP301S transgenic mouse brains. Note that mitophagic accumulation is not readily detected in non-transgenic (non-Tg) littermate brains. (**D**) Quantitative analysis was expressed as the percentage of morphologically abnormal mitochondria with swollen shape and loss of cristae integrity (asterisks) per neuronal perikarya and the average number of mitochondria within autophagic vacuole-like organelles (arrows) in the cross-section (10 × 10 μm). 'N' indicates the nucleus in the neuronal soma. (**E** and **F**) Representative blots (**E**) and quantitative analysis (**F**) and showing increased recruitment of Parkin and p62 to mitochondria along with a reduction in Miro1 levels in tauP301L transgenic mouse brains. Note that phospho-tau is localized to mitochondria in tauP301L mouse brains. Following Percoll-gradient membrane fractionation, equal amounts (5 μg) of mitochondria-enriched membrane fractions (Mito) and post-nuclear supernatants (PNS) from the cortices of non-transgenic littermate and tauP301L transgenic mouse brains were sequentially immunoblotted with antibodies against mitophagy markers Parkin and p62, mitochondrial proteins TOM20, SOD2 and HSP60, and cytosolic protein GAPDH, along with hyperphosphorylated tau (AT8 and PHF1). The purity of Mito fractions was confirmed by the relative enrichment of mitochondrial markers TOM20, SOD2 and HSP60 and by the absence of GAPDH, compared to those in post-nuclear supernatant fractions. The intensities of proteins in Mito fractions purified from tauP301L transgenic mouse brains were normalized to those in non-transgenic littermate controls (**F**). Data were quantified from three independent repeats. (**G** and **H**) Quantitative analysis (**G**) and representative blots (**H**) showing increased levels of Parkin, LC3-II and p62 along with decreased Miro1 in Mito fractions isolated from FTD patient brains. The intensities of proteins in Mito fractions purified from FTD patient brains were normalized to those in normal control subjects (**G**). Data were quantified from three independent repeats (**G**) and from total numbers of slice sections and neurons and mitochondria (*n*) as indicated in parentheses (**B** and **C**). Scale bars = 100 nm (**D**) and 10 μm (**A**). Error bars represent SEM. Student's *t*-test: $^{***}P < 0.001$; $^{**}P < 0.01$.

data are in accord with the results from light imaging studies, supporting the view that mitophagy is extensively activated at the early disease stages of tauopathy.

Given that Parkin-mediated mitophagy is the best-understood pathway in which Parkin translocates from the cytoplasm onto damaged mitochondria to facilitate their sequestration

within autophagosomes,[16,20–23] we further determined whether Parkin-mediated mitophagy is activated in tauopathy brains. We isolated mitochondria-enriched fractions (Mito) from the brains of a tauopathy mouse model and FTD patient brains. The purity of Mito fractions was confirmed by the relative mitochondrial enrichment of mitochondrial protein markers TOM20, SOD2, and VDAC1 or HSP60 and by the absence of cytosolic protein glyceraldehyde 3-phosphate dehydrogenase (GAPDH), relative to those in post-nuclear supernatant fractions. When equal amounts of Mito and post-nuclear supernatant fractions were loaded, the levels of mitophagy markers Parkin and p62 were drastically elevated in Mito fractions purified from tauP301L transgenic mouse brains as compared to those of non-transgenic littermate controls (Fig. 3E and F). Furthermore, mitochondria purified from FTD patient brains also exhibit a markedly increased association with Parkin, p62 and LC3-II relative to those of normal control subjects (Fig. 3G and H). Consistent with the results from confocal imaging and TEM studies, the biochemical evidence from both the brains of the tauopathy mouse model and post-mortem patients further suggests that Parkin-mediated mitophagy is markedly activated.

To assess Parkin-mediated mitophagy, we performed additional lines of experiments. We first examined ubiquitin phosphorylation at serine 65 (pS65-Ub), an indicator of activation of PINK1/Parkin-mediated mitophagy.[52–55] The fluorescence intensity of pS65-Ub, which appeared as vesicular structures and co-localized with cytochrome *c*-labelled mitochondria, was significantly increased in the soma of hippocampal neurons in tauP301L transgenic mouse brains as compared to that of non-transgenic littermate controls (Supplementary Fig. 3C and D). Moreover, pS65-Ub was elevated at the early disease stage (4 months of age) and over disease progression at the age of 8 and 12 months in tauP301L mouse brains relative to non-transgenic littermate controls (Supplementary Fig. 3E). We next measured Parkin-mediated mitophagic flux in primary cortical neurons derived from tauP301S transgenic mouse brains by utilizing Bafilomycin A1 (Baf-A1), an inhibitor widely used in the field that blocks autophagosome–lysosome fusion and suppresses lysosomal degradation.[56] In line with drastic activation of Parkin-mediated mitophagy in the brains of FTD patients and tauopathy mice (Fig. 3E–H), we detected an increase in the percentage of tauP301S transgenic neurons with mitochondria targeted by Parkin under the basal condition, which was augmented after Baf-A1 treatment (Supplementary Fig. 3F and G). Moreover, tauP301S neurons exhibited a higher increase relative to non-transgenic littermate control neurons in the presence of Baf-A1, suggesting that Parkin-mediated mitophagic flux is enhanced in tauopathy neurons. The data were consistent with the biochemical analysis showing a robust elevation of LC3-II levels in tauopathy neurons incubated with Baf-A1 (Supplementary Fig. 3H and I). Therefore, these observations collectively support the notion that Parkin-mediated mitophagy is broadly activated in tauopathy neurons.

In Mito fractions isolated from FTD patient brains and tauopathy mouse model, we detected increased phospho-tau levels as visualized by AT8 and/or PHF1 antibodies (Fig. 3E and H), suggesting that phospho-tau is abnormally localized to mitochondria. This observation is consistent with previous studies and supports the notion that phospho-tau induces mitochondrial toxicity through its association with mitochondria.[9,10,12,14–16,57] Our results further suggest that phospho-tau–mediated insults to mitochondria likely trigger extensive mitophagy activation in early tauopathy. Interestingly, we found a marked reduction in Miro1 proteins on mitochondria purified from the brains of tauopathy mice and FTD patients (Fig. 3E–H). However, the mRNA levels of Miro1 are not altered in tauopathy brains (Supplementary Fig. 3J and K). Miro1 is anchored to the mitochondrial outer membrane and acts as a KIF5 receptor, essential for anterograde transport of mitochondria.[21] It is well established that Miro1 is a substrate of Parkin E3 ubiquitin ligase and Parkin targets Miro1 for degradation through the proteasome system upon mitophagy induction.[29–32] Thus, Miro1 reduction in tauopathy brains is likely attributed to Parkin-enhanced Miro1 turnover, impairing Miro1-mediated mitochondrial anterograde transport towards tauopathy synapses.

Parkin activation accelerates Miro1 degradation and thereby arrests mitochondrial anterograde movement in tauopathy axons

Therefore, we tested whether defective anterograde transport of mitochondria in tauopathy axons is caused by loss of Miro1. Strikingly, overexpression of Miro1 in tauP301S transgenic neurons remarkably increases mitochondrial anterograde movement (Fig. 4A and B). Moreover, Miro1-enhanced anterograde transport raises mitochondrial supply to tauP301S axons, as reflected by an increase in the number of mitochondria. The data suggest that increasing Miro1 levels reverses impeded mitochondrial anterograde movement and rescues mitochondrial distribution deficits in distal tauopathy axons. Similar effects can be detected in axons expressing tauP301L (Supplementary Fig. 4A and B). These results indicate that defects in mitochondrial anterograde transport in tauopathy axons can be attributed to decreased Miro1.

We next determined whether the reduction in Miro1 levels is the result of increased Miro degradation in tauopathy neurons upon activation of the Parkin pathway. We and others have demonstrated that Parkin-mediated mitophagy can be induced in neurons treated with carbonyl cyanide *m*-chlorophenylhydrazone (CCCP), an $\Delta\psi_m$ uncoupler.[24,28,31,35,58] Thus, we examined whether acute $\Delta\psi_m$ dissipation augments Miro1 reduction in tauopathy neurons. Following CCCP treatment, tauP301S transgenic neurons display increased LC3-II and decreased Miro1. It is important to note that tauP301S transgenic neurons exhibit more pronounced changes as compared to non-transgenic control neurons (Fig. 4C and D and Supplementary Fig. 4C). This result indicates that while $\Delta\psi_m$ dissipation triggers Parkin-induced Miro1 degradation in both non-transgenic and tauP301S transgenic neurons, such an effect is more robust in tauP301S neurons.

Upon mitophagy activation, Parkin translocates onto depolarized mitochondria and functions as an E3 ubiquitin ligase, inducing Miro1 degradation through the proteasome system.[28–32] We next purified mitochondrial fractions from tauP301S transgenic neurons to assess whether elevated Miro1 turnover is coupled with increased Parkin association with mitochondria following dissipating $\Delta\psi_m$. In tauP301S neurons, we detected depletion of Miro1 on mitochondria, accompanied by enhanced recruitment of Parkin along with p62 and LC3-II to mitochondria (Fig. 4E). Our data suggest that reduced Miro1 levels in tauopathy neurons can be attributed to Parkin activation-induced Miro1 degradation after Parkin is recruited to mitochondria. We further examined Parkin association with mitochondria in live tauP301S neurons in the presence and absence of CCCP. TauP301S neurons consistently show increased Parkin localization to mitochondria under the basal condition, relative to that in non-transgenic controls (Fig. 4F and G and Supplementary Fig. 4D). Moreover, $\Delta\psi_m$ dissipation leads to a higher increase in the percentage of tauP301S neurons showing Parkin translocation onto mitochondria than that in non-transgenic neurons (Fig. 4F and G and Supplementary Fig. 4D). Thus, the imaging data are in accord with the biochemical results (Fig. 4C and D and Supplementary Fig. 4C) and suggest that tauopathy neurons exhibit more efficient Parkin recruitment to mitochondria upon mitochondria damage.

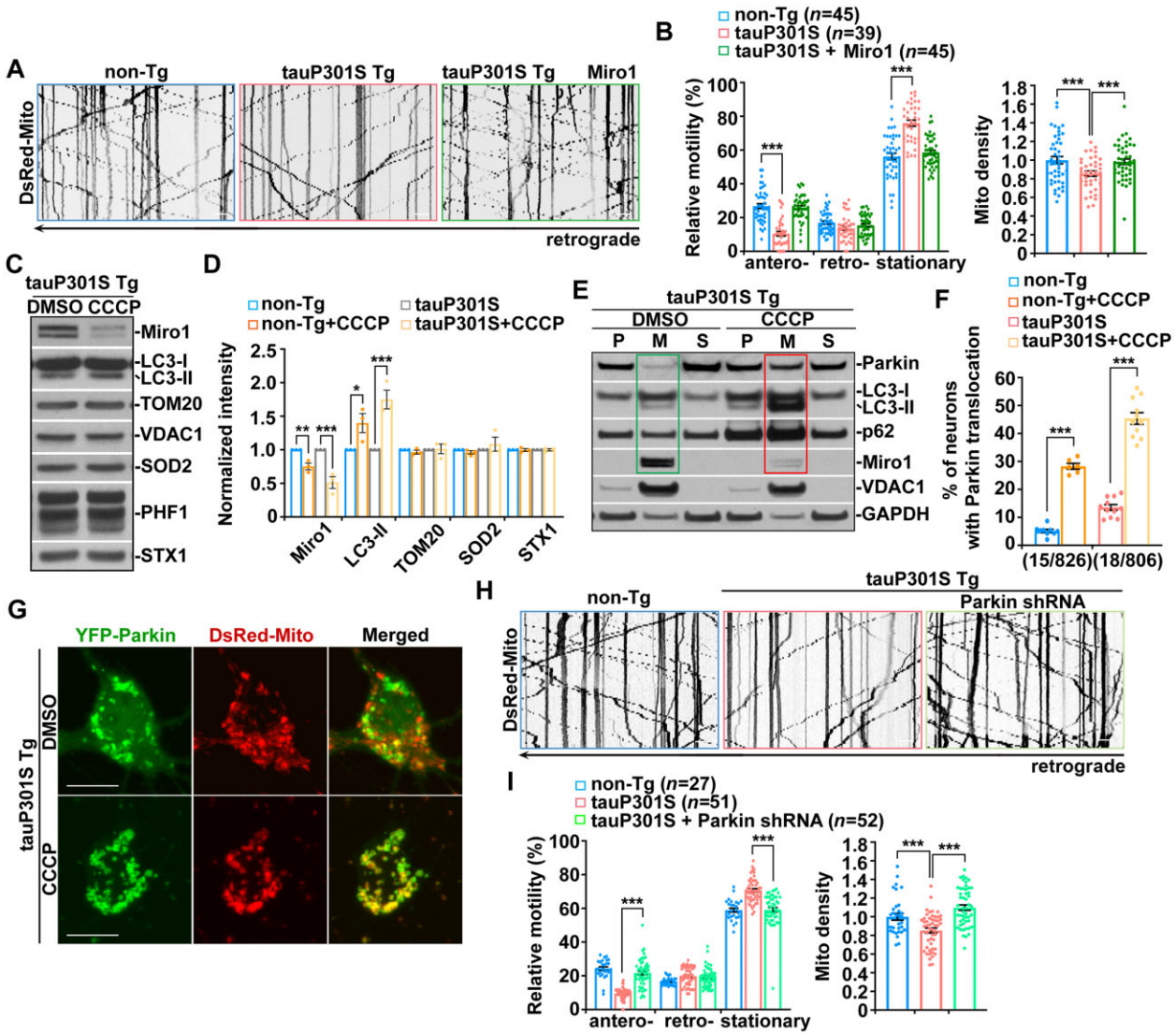

Figure 4 Parkin activation accelerates Miro1 degradation and thereby arrests mitochondrial anterograde movement in tauopathy axons. (**A** and **B**) Representative kymographs (**A**) and quantitative analysis (**B**) showing that elevated Miro1 expression reverses mitochondrial anterograde movement and restores mitochondrial distribution in the axons of tauP301S neurons. (**C** and **D**) $\Delta\psi_m$ dissipation augments mitophagy accompanied by enhanced Miro1 degradation in tauP301S transgenic (Tg) neurons. Note that tauP301S neurons exhibit a stronger response to CCCP treatment than that of non-transgenic (non-Tg) littermate controls. Non-transgenic or tauP301S transgenic neurons were incubated with DMSO or 10 μM CCCP for 24 h. A total amount of 20 μg cortical neuron lysates was sequentially detected on the same membrane with antibodies as indicated. Changes in protein intensities were normalized by that of neuronal protein syntaxin-1 (STX1) and compared to dimethyl sulphoxide (DMSO)-treated controls. Data were quantified from three independent repeats. (**E**) Representative blots showing depletion of Miro1 along with increased levels of Parkin, LC3-II and p62 in mitochondria-enriched membrane fractions purified from tauP301S neurons following dissipating $\Delta\psi_m$. TauP301S neurons were incubated with DMSO or 10 μM CCCP for 24 h and then subjected to fractionation into post-nuclear supernatant (P), mitochondrial fraction (M) and cytosolic supernatant (S). Equal amounts of protein (10 μg) were sequentially immunoblotted with antibodies against Parkin, p62 and LC3-II, mitochondrial protein VDAC1, and cytosolic protein GAPDH on the same membranes after stripping between each antibody application. (**F** and **G**) Parkin recruitment to mitochondria is augmented in tauP301S neurons upon CCCP treatment. The percentage of non-transgenic and tauP301S transgenic neurons in the presence and absence of CCCP showing Parkin translocation onto mitochondria was quantified, respectively. (**H** and **I**) Increased anterograde transport of mitochondria in tauP301S transgenic axons expressing Parkin shRNA. Note that mitochondrial retrograde movement remains unaffected in tauP301S axons. Data were quantified from a total number of neurons as indicated in parentheses (**B**, **F** and **I**) from at least three independent experiments. Scale bars = 10 μm. Error bars represent SEM. Student's *t*-test: $^{***}P < 0.001$; $^{*}P < 0.05$.

To examine this model further, we assessed whether Parkin RNAi in tauopathy neurons reverses impeded anterograde transport of mitochondria, mimicking an effect of elevated Miro1 expression (Fig. 4A and B). Interestingly, after expressing Parkin shRNA as previously described,[58,59] we detected a significant increase in mitochondrial anterograde movement along tauP301S axons (Fig. 4H and I). Consistent with the results from Miro1 elevation (Fig. 4A and B), enhanced mitochondrial anterograde transport was accompanied by an increased number of mitochondria in tauP301S axons following Parkin RNAi (Fig. 4H and I), suggesting that defective mitochondrial anterograde movement is Parkin-dependent. Autophagy receptors NDP52 and optineurin (OPTN) were reported to be required for PINK1/Parkin-dependent mitophagy.[60–63] However, both NDP52 RNAi and OPTN RNAi failed to restore impaired mitochondrial anterograde transport in tauP301S axons (Supplementary Fig. 4E and F). The data indicate that blocking Parkin but not mitophagy downstream of Parkin activation rescues mitochondrial defects in tauopathy axons. Together with the

results from tauopathy brains (Fig. 3E–H) and neurons in culture (Supplementary Fig. 3C–I), these findings support the view that broad activation of the Parkin pathway triggers excessive Miro1 degradation and consequently hampers Miro1-mediated anterograde transport of mitochondria in tauopathy axons.

To gain further mechanistic insights into enhanced Miro1 turnover linked to tauopathy, we performed additional lines of experiments and determined whether such a defect is related to the burden of phospho-tau. HEK293 cells expressing GFP-tauP301L, but not GFP control, show accumulation of phospho-tau labelled by AT8 antibody. Interestingly, these cells exhibit a significant reduction in endogenous Miro1, but not Trak1 (Supplementary Fig. 4G and H). Trak1, a component of the Miro1-Trak1-KIF5 adaptor–motor complex, is not subject to mitophagy-induced degradation.[12,16,21] We further tested a dose-dependent effect and found gradually decreased Miro1 coupled with an increased burden of phospho-tau in cells transfected with an increasing amount of GFP-tauP301L plasmid (Supplementary Fig. 4I and J). Trak1 consistently shows no significant change. The data suggest that excessive Miro1 turnover is an effect of phospho-tau accumulation.

Tauopathy neurons exhibit a stronger mitophagy response to $\Delta\psi_m$ dissipation (Fig. 4C and D and Supplementary Fig. 4C). Moreover, we have demonstrated that phospho-tau is associated with mitochondria (Fig. 3E and H) and has a dose-dependent effect on Miro1 turnover (Supplementary Fig. 4C–J). These observations suggest the possibility that mitochondria with phospho-tau burden are more susceptible to Parkin-mediated mitophagy, thereby augmenting Miro1 degradation. We next determined whether phospho-tau interacts with Parkin. Indeed, we detected the phospho-tau-Parkin complex in transfected HeLa cells expressing tauP301L and Parkin (Supplementary Fig. 4K). AP/tauP301L was used as an internal control in which 14 serine (S) and threonine (T) residues were changed to non-polar alanine and proline residues, termed AP for alanine–proline, to prevent phosphorylation.[64] This result indicates that phospho-tau, but not tauP301L, forms a complex with Parkin. Together, these findings allow us to propose that, by interacting with Parkin, mitochondria localized phospho-tau promotes Parkin translocation from cytoplasm onto mitochondria, thus accelerating Miro1 degradation in tauopathy neurons.

Increasing Miro1 levels enhances mitochondrial supply to tauopathy synapses and ameliorates synaptic failure

We next determined whether deficits in the synaptic distribution of mitochondria are caused by activation of Parkin but not the downstream of mitophagy in tauopathy neurons. We found increased mitochondrial distribution at the SYP-labelled presynaptic terminals and in the axons of tauP301S transgenic neurons lacking Parkin, but not NDP52 or OPTN (Supplementary Fig. 5A and B). This result is consistent with the rescue effect of Parkin RNAi on impaired mitochondrial anterograde transport in tauopathy axons (Fig. 4H and I and Supplementary Fig. 4E and F) and further indicates that loss of Parkin, but not blocking mitophagy downstream of Parkin, elevates mitochondrial supply to tauopathy synapses. Thus, these findings collectively support our model that Parkin activation induces synaptic mitochondrial deficits by accelerating Miro1 turnover and thus disrupting Miro1-mediated mitochondrial anterograde transport towards tauopathy synapses.

Given Miro1 elevation induced beneficial effects against defects in mitochondrial anterograde transport and distribution in tauopathy axons (Fig. 4A and B and Supplementary Fig. 4A and B), we next examined whether mitochondrial populations at tauopathy synapses can also be restored after increasing Miro1 levels. In line with our results from the brains of patients with tauopathies and mouse models (Fig. 1), tauP301S transgenic neurons displayed a reduction in mitochondrial distribution at presynaptic terminals, accompanied by the decreased density of presynaptic boutons along axons (Fig. 5A and B). Importantly, elevating Miro1 remarkably raises the presynaptic distribution of mitochondria as well as the density of presynaptic boutons in tauP301S neurons (Fig. 5A and B). Moreover, overexpression of Miro1 attenuates mitochondrial stress in tau axons as reflected by a decrease in oxidatively damaged mitochondria (Supplementary Fig. 5C–E). Our data suggest that Miro1-enhanced anterograde transport facilitates the delivery of healthy mitochondria towards tauopathy axons. Consistent with increased mitochondrial supply and reduced mitochondrial stress in axons and at synapses following Miro1 elevation (Figs 4A, B, 5A and B and Supplementary Fig. 5D and E), we further observed a drastic increase in cellular ATP levels in tauP301S neurons expressing AT1.03, particularly within the axons as indicated by elevated cellular YFP/CFP ratios (Supplementary Fig. 5F and G). More robust increases in ATP levels within tauopathy axons further support the view that Miro1-enhanced mitochondrial anterograde movement alleviates energy deficits by increasingly supplying healthy mitochondria to axons and synaptic terminals.

Synaptic dysfunction has been linked to early pathophysiology in tauopathy.[46] We next examined whether the enhanced supply of healthy mitochondria and the amelioration of energy deficits rescue synaptic damage in tauopathy neurons after increasing Miro1 levels. We determined functional release sites by measuring FM4-64 dye [*N*-(3-triethylammoniumpropyl)-4-(6-(4-(diethylamino) phenyl) hexatrienyl) pyridinium dibromide]–labelled synaptic vesicles. FM dye at presynaptic boutons is taken up in an activity-dependent manner, and the majority of GFP-SYP-labelled presynaptic terminals can be marked by FM4-64 (Fig. 5C and D) , which represents active synapses. Compared to non-transgenic littermate controls, tauP301S transgenic neurons exhibit marked reductions in the number of FM dye puncta per 100 μm axonal processes and the percentage of active synapses. These findings are in accord with reduced SYP density along axons (Fig. 5A and B), and further suggest defects in synaptic vesicle recycling or release at tauP301S synapses. Excitingly, overexpression of Miro1 increases both the number and the percentage of functional release sites along tauP301S axons (Fig. 5C and D), indicating a beneficial effect of Miro1 elevation against synaptic damage associated with tauopathy.

To examine the protective effects of Miro1 elevation on tauopathy-associated synaptic damage at a functional level, we performed a whole-cell patch-clamp to record miniature (mini) excitatory postsynaptic currents (mEPSCs) in cultured cortical neurons transfected with GFP, GFP-tauP301L, or GFP-tauP301L and Miro1 (Fig. 5E). We specially chose to record mEPSCs in untransfected postsynaptic neurons with no GFP signals but were surrounded by the GFP-positive presynaptic neurons expressing GFP only, GFP-tauP301L, or GFP-tauP301L and Miro1, as previously described.[64–68] Given that the majority of the presynaptic inputs of untransfected postsynaptic neurons originated from surrounding transfected presynaptic neurons with GFP signals, we thus attributed any changes in mEPSCs recorded from untransfected postsynaptic neurons to the modulation of presynaptic activities by the presynaptic neurons expressing tauP301L. Compared to GFP controls, the mean frequency of mEPSCs is significantly decreased in the non-transfected postsynaptic neurons surrounded by the presynaptic neurons expressing GFP-tauP301L (Fig. 5E and F). Decreases in mEPSC frequency are consistent with reduced densities of presynaptic terminals and active synapses (Fig. 5A–D), suggesting synaptic failure in tauP301L-expressed neurons. Strikingly, elevated Miro1 expression rescues such a defect by increasing mEPSC frequency to 1.34 ± 0.24 Hz (Fig. 5E and F).

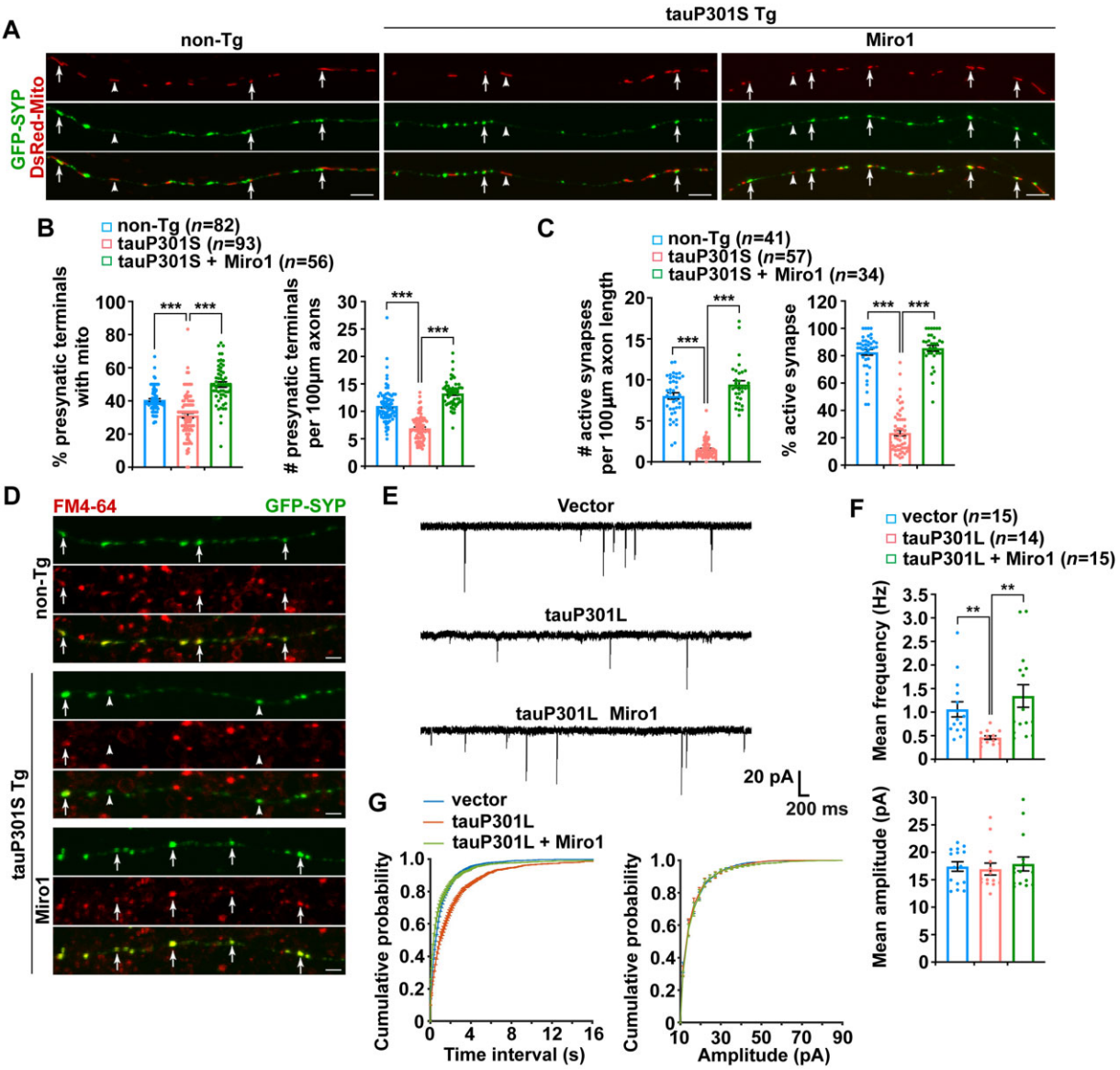

Figure 5 Increasing Miro1 levels enhances mitochondrial supply to tauopathy synapses and ameliorates synaptic failure. (**A** and **B**) Representative images (**A**) and quantitative analysis (**B**) showing that overexpression of Miro1 elevates mitochondrial supply to presynaptic terminals labelled by SYP, as well as the density of synapses along tauP301S axons. Data were expressed as the percentage of presynaptic terminals with mitochondria and the number of SYP puncta per 100 μm axonal length, respectively. (**C** and **D**) Quantitative analysis (**C**) and representative images (**D**) showing that increasing Miro1 expression in tauP301S neurons raises the density of active presynaptic terminals taking up FM4-64, as evidenced by increased FM4-64 puncta within tauP301S axons. Quantification data were expressed as the number of FM4-64 puncta per 100 μm axonal length and the percentage of active synaptic sites co-labelled by FM4-64 and SYP, respectively. (**E**–**G**) Representative miniature excitatory postsynaptic currents (mEPSCs) (**E**) recorded from the non-transfected postsynaptic neurons with no GFP signals surrounded by the presynaptic neurons expressing GFP, GFP-tauP301L, or GFP-tauP301L and myc-Miro1. Note that the frequency of mEPSCs is higher in the non-transfected postsynaptic neurons surrounded by the presynaptic neurons expressing GFP or GFP-tauP301L and Miro1, as compared to neurons surrounded by the presynaptic neurons expressing GFP-tauP301L (**E**). Cultured cortical neurons transfected with GFP, GFP-tauP301L, or GFP-tauP301L and myc-Miro1, and mEPSCs were recorded at DIV14–18 in the presence of 1 μM TTX and 100 μM PTX. Bar graphs of mean frequencies and mean amplitudes (**F**) and cumulative probability plots of inter-event intervals and mEPSC amplitude (**G**) recorded from neurons in (**E**) are presented. Presynaptic expressing GFP-tauP301L exhibits fewer mEPSCs recorded from the non-transfected postsynaptic neurons, relative to presynaptic expressing GFP or GFP-tauP301L and myc-Miro1 (**F**). There is a significant increase in the inter-event interval of mEPSCs in the presynaptic neurons expressing tauP301L, which is reversed by overexpression of Miro1 (**G**). The Mann–Whitney U-test/Wilcoxon rank sum test was used. Data were quantified from a total number of neurons as indicated in parentheses (**B**, **C** and **F**) from at least three independent experiments. Scale bars = 10 μm. Error bars represent SEM. Student's *t*-test: $^{***}P < 0.001$; $^{**}P < 0.01$. non-Tg = non-transgenic; Tg = transgenic.

Furthermore, consistent with a comparable reduction in mEPSC frequency, cumulative frequency distribution of inter-event intervals further revealed rightward shifts for the untransfected postsynaptic neurons surrounded by the presynaptic neurons expressing GFP-tauP301L, which are reversed by overexpression of Miro1 (Fig. 5G). We did not observe any change in the amplitude of mEPSCs, suggesting unaltered postsynaptic glutamate receptors in the recorded non-transfected postsynaptic neurons. Consistent with our imaging data, these electrophysiological results suggest that increasing Miro1 levels rescues impaired synaptic function by increasing mitochondrial supply and attenuating energy deficits at tauopathy synapses.

Miro1-enhanced mitochondrial anterograde transport restores healthy mitochondrial populations at synaptic terminals

The *in vitro* rescue effects of elevated Miro1 expression in cultured tauopathy neurons led us to further determine the *in vivo* effects in tauopathy mouse brains by bilateral injection of AAV-mCherry-Miro1 into the hippocampus and the cortex, an established *in vivo* delivery procedure by us and others.[43,58,69–73] We injected two different tauopathy mouse models (tauP301L transgenic (rTg4510) and tauP301S transgenic (PS19) lines), and assessment of AAV-injected mice revealed widespread brain expression, particularly in hippocampal (Supplementary Fig. 6). We first verified Miro1 expression in mitochondrial fractions purified from the hippocampi of AAV-injected mouse brains by western blot analysis. Miro1 expression on mitochondria is significantly increased in tauP301L transgenic mouse brains at the age of 6–7 months after injection with AAV-mCherry-Miro1 (Fig. 6A and B), relative to that of control tauP301L mouse brains expressing AAV-mCherry. Moreover, mitochondria with elevated Miro1 expression exhibit reduced PHF1-labelled phospho-tau, suggesting the possibility that these mitochondria represent a newly generated healthy population with less phospho-tau burden. To test this possibility, we measured the OCR in mitochondria freshly isolated from the hippocampi of non-transgenic and tauP301L transgenic mice with and without Miro1 injection. Indeed, basal, maximal and ATP-linked respiration rates in mitochondria were significantly elevated in tauP301L mouse brains as compared to those of control tau mice injected with AAV-mCherry (Fig. 6C). Given the fact that mitochondrial biogenesis occurs mostly in the soma of neurons,[21,74] these *in vivo* effects of Miro1 overexpression are in line with the observations in cultured tauopathy neurons showing decreases in oxidatively damaged mitochondria coupled with increases in mitochondrial energetic activity within axons (Supplementary Fig. 5), supporting the view that increasing Miro1 levels enhances the delivery of healthy mitochondrial populations towards tauopathy axonal terminals.

Next, we assessed whether Miro1-enhanced mitochondrial anterograde transport restores synaptic mitochondrial populations in tauopathy mouse brains. While tauP301L transgenic mouse brains consistently exhibit deficits in the synaptic distribution of mitochondria, we detected remarkable increases in the levels of mitochondrial proteins in synapse-enriched synaptosomal preparations purified from the brains of tauP301L transgenic mice injected with AAV-mCherry-Miro1 as compared to those of control tau mice expressing mCherry (Fig. 6D and E). This result suggests that elevated Miro1 expression effectively increases the supply of mitochondria to synaptic terminals in mouse brains after AAV

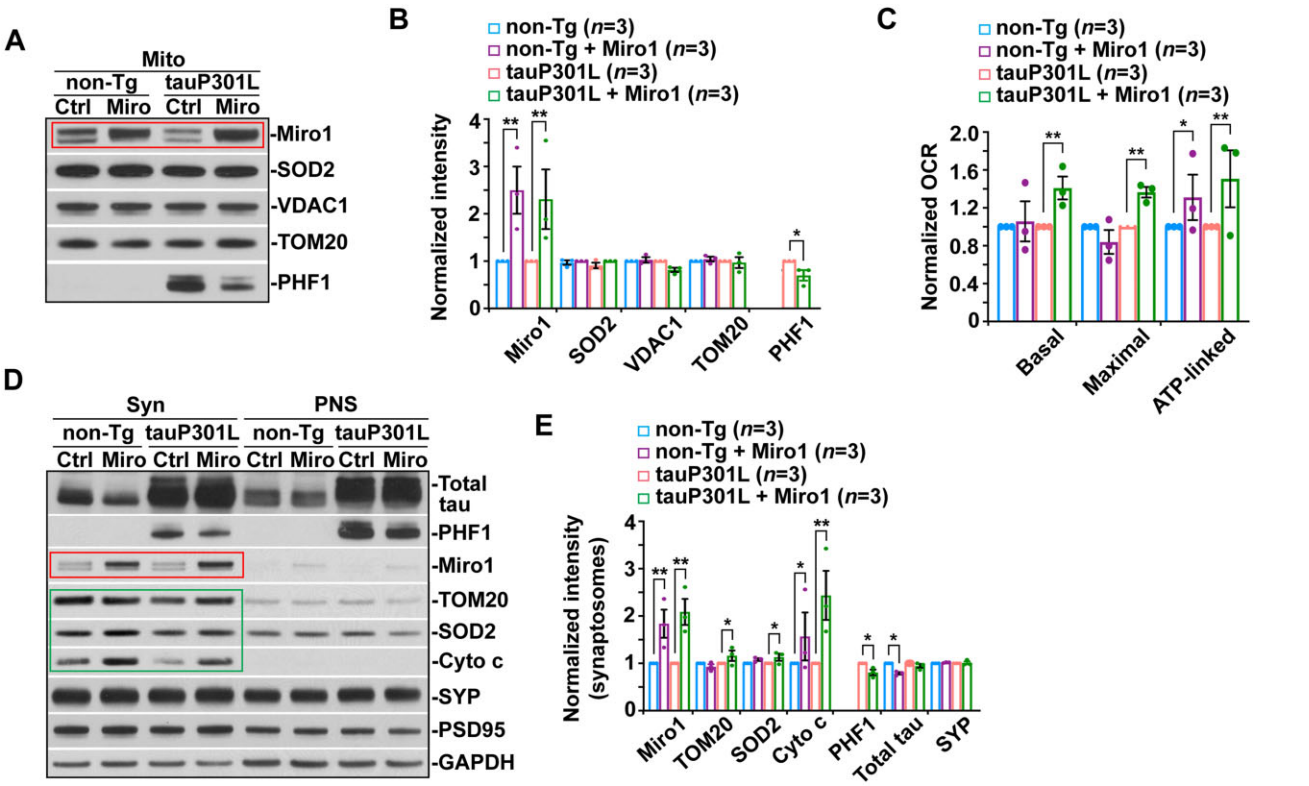

Figure 6 Miro1-enhanced mitochondrial anterograde transport restores healthy mitochondrial populations at synaptic terminals in tauopathy mouse brains. (**A** and **B**) Representative blots (**A**) and quantitative analysis (**B**) showing increased Miro1 levels on mitochondria in the hippocampus of non-transgenic (non-Tg) and tauP301L transgenic (Tg) mouse brains injected with AAV-mCherry-Miro1. Note that phospho-tau levels are decreased in mitochondrial (Mito) fractions purified from tauP301L mouse brains with Miro1 injection. The intensities of proteins in Mito fractions were normalized to those in non-transgenic or tauP301L mice expressing AAV-mCherry control (**B**), respectively. Data were quantified from three independent repeats. (**C**) Attenuation of impaired mitochondrial function in tauP301L transgenic mouse brains after overexpression of Miro1. Seahorse mitochondrial stress assay using freshly isolated cortical and hippocampal mitochondria from tauP301L transgenic mouse brains transduced with AAV-mCherry-Miro1 display significant increases in basal, maximal and ATP-linked respiration rates. OCR measurements of mitochondria purified from AAV-mCherry-Miro1–injected mouse brains were normalized to those from non-transgenic or tauP301L mice expressing AAV-mCherry control, respectively. Data were quantified from three independent repeats. (**D** and **E**) Restored supply of mitochondria along with a reduction in phospho-tau levels at synaptic terminals in the hippocampus of 6–7-month-old tauP301L mouse brains expressing AAV-mCherry-Miro1. The protein intensities in synaptosomal (Syn) fractions were normalized to those in non-transgenic or tauP301L mice expressing AAV-mCherry (**E**). Data were quantified from three independent repeats. Error bars represent SEM. Student's *t*-test: $^{***}P < 0.001$; $^{**}P < 0.01$; $^{*}P < 0.05$.

injection, a finding consistent with the observations in cultured tauP301S transgenic neurons (Fig. 5A and B). Importantly, similar to our data from isolated mitochondrial fractions (Fig. 6A and B), the levels of phospho-tau, but not total tau, are decreased in synaptosomal preparations purified from tauP301L mouse brains transduced with AAV-mCherry-Miro1 (Fig. 6D and E). Together with the results from cultured tau neurons and the OCR measurement of mitochondria freshly isolated from AAV-injected tauP301L mouse brains (Supplementary Fig. S5 and Fig. 6C), these findings indicate that Miro1-enhanced mitochondrial anterograde movement corrects deficits in mitochondrial distribution at tauopathy synapses.

Miro1-increased synaptic mitochondrial supply attenuates synaptic defects and alleviates neuronal death

We further determined whether increases in synaptic healthy mitochondrial populations and energy supply protect against synaptic pathology in tauopathy mouse brains. Compared to non-transgenic littermate mice, we found that both the area and the mean intensity of SYP-labelled presynaptic terminals were significantly reduced in the hippocampal mossy fibre regions of tauP301L transgenic mice at the age of 6–7 months (Fig. 7A and B), suggesting synapse loss in tauP301L mouse brains. Strikingly, such a defect is remarkably attenuated in tauP301L transgenic mouse brains injected with AAV-mCherry-Miro1. In tauP301S transgenic mouse brains at 9 months of age, we detected similar rescue effects (Supplementary Fig. 7A and B). These *in vivo* results along with biochemical evidence are in accord with the findings in cultured tau neurons (Figs 5 and 6 and Supplementary Fig. 5), collectively indicating that Miro1-enhanced mitochondrial anterograde transport counteracts tauopathy-associated synaptic defects by supplying healthy mitochondrial populations to tauopathy synapses. We further examined whether increasing Miro1 expression has a beneficial effect against neuron death in tauopathy mouse brains. Our data are consistent with previous studies from other groups,[7,70] and show that tauP301L transgenic mice exhibit decreased neuron density in the hippocampal CA1 regions, relative to non-transgenic littermate controls (Fig. 7C and D). Importantly, overexpression of Miro1 prevents neuron loss, as evidenced by an increased number of NeuN-positive neurons in this region of tauP301L mouse brains. In addition, mitophagy was not altered in tauopathy mouse brains with elevated expression of Miro1, as evidenced by no detectable change in mitophagosome density relative to control tauopathy mouse brains injected with AAV-mCherry (Supplementary Fig. 7C and D). Thus, the *in vivo* evidence from tauopathy mouse brains suggests that Miro1-enhanced supply of healthy mitochondria prevents tauopathy-associated synaptic defects and neurodegeneration.

Elevated Miro1 expression improves behavioural performance and synaptic function in tauopathy mice

Given Miro1-mediated rescue effects on synaptic defects in tauopathy mouse brains (Fig. 7 and Supplementary Fig. 7), we speculated that increasing Miro1 expression ameliorates learning and memory deficits in tauopathy mice. We asked whether elevated Miro1 expression prevents these behavioural abnormalities,

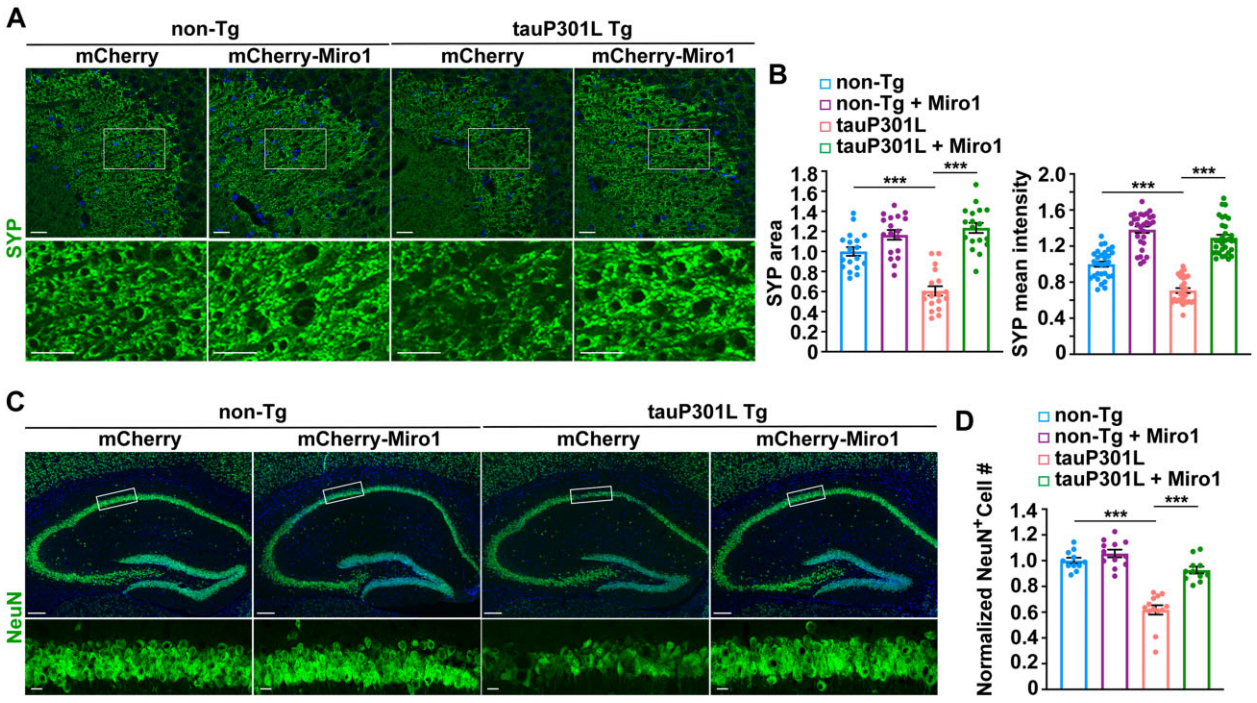

Figure 7 Miro1-increased synaptic mitochondrial supply attenuates synaptic defects and alleviates neurodegeneration in tauopathy mouse brains. (**A** and **B**) Representative images (**A**) and quantitative analysis (**B**) showing that increasing Miro1 expression prevents loss of presynaptic terminals in the hippocampal mossy fibres of tauP301L transgenic (Tg) mouse brains at the age of 6–7 months. The area and the mean intensity of SYP-marked presynaptic terminals were quantified and normalized to those of non-transgenic (non-Tg) mice infected with AAV-mCherry, respectively (**B**). (**C** and **D**) Representative images (**C**) and quantitative analysis (**D**) showing that overexpression of Miro1 protects against neuron death in the hippocampal CA1 regions of tauP301L transgenic mouse brains. The number of NeuN-labelled neurons in hippocampal CA1 areas marked by rectangles was quantified and normalized to that of non-transgenic mice expressing AAV-mCherry. Data were quantified from a total number of 35–40 imaging slice sections in non-transgenic and tauP301L transgenic mouse brains with AAV injection, respectively. Scale bars = 25 μm (**A** and *bottom* panel in **C**); 250 μm (*top* panel in **C**). Error bars represent SEM. Student's *t*-test: ***$P < 0.001$.

which are readily detectable in tauP301S transgenic mice. In the open field test, 6-month-old tauP301S transgenic mice displayed greater locomotion and less anxiety-like behaviour. This was evidenced by increased travel distance in the open field and more time spent in the field centre, an indication of reduced anxiety. This suggests that tauopathy mice were more hyperactive (Supplementary Fig. 8B), a finding in agreement with previous studies.[45,75,76] Following AAV-mediated Miro1 overexpression, there was no significant effect on the hyperactivity of tauP301S mice (Supplementary Fig. 8B). Phospho-tau accumulation in the prefrontal cortex and amygdala was proposed to induce hyperactive behaviour.[41,77,78] Thus, our results suggest the persistence of brain regions driving hyperlocomotor behaviour, which is resistant to Miro1 modulation.

We next performed the three-chamber test to examine sociability and social recognition memory.[45,79–81] Animals with normal sociability show a preference for the chamber with a stranger mouse over an empty chamber, a phenomenon indicated by greater time spent in the stranger chamber. TauP301S transgenic mice showed comparable social interaction as non-transgenic littermate controls (Fig. 8A). During the social novelty preference/recognition test that requires normal hippocampal function, non-transgenic mice spent significantly longer time exploring the chamber containing a novel, stranger mouse. However, tauP301S transgenic mice failed to distinguish the stranger mouse from the familiar mouse and spent similar time with the stranger mouse relative to the familiar mouse (Fig. 8B). Our observations are consistent with previous studies,[45] suggesting that this tauopathy mouse model has impaired social memory. Importantly, elevated Miro1 expression in tauP301S transgenic mice significantly reverses this phenotype, as reflected by more time spent with the stranger mouse (Fig. 8B). Thus, these results indicate that Miro1-enhanced anterograde mitochondrial transport attenuates defects in tauopathy-associated social recognition memory.

To assess spatial learning and memory, we conducted the Morris water maze test in 7-month-old tauP301S transgenic mice and non-transgenic littermates injected with AAV-mCherry-Miro1 or AAV-mCherry control. Mice were trained to find a hidden platform across three training blocks (Blocks 2–4) on a single day and with each block involving 3–4 acquisition trials, followed by memory testing in a 60-s probe trial at an hour after the last hidden-platform training.[82,83] Block 1 involved a flagged, visible platform to establish escape behaviour. Non-transgenic mice with or without Miro1 expression displayed similar latency to find the platform during the hidden-platform training phase and favoured the target quadrant in the probe trial (non-transgenic versus non-transgenic + Miro1; Fig. 8C and D), indicating that elevated Miro1 expression caused no adverse effects in learning and memory in non-transgenic mice. In contrast, tauP301S transgenic mice performed poorly in both the acquisition phase and the memory probe tests, as evidenced by longer latency on training blocks 3 and 4 and less path length and less time in the target quadrant (non-transgenic versus tauP301S transgenic). However, AAV-mediated Miro1 overexpression significantly improved learning and enhanced memory retention in tauP301S mice that showed no detectable difference from non-transgenic mice (Fig. 8C and D). Therefore, elevated Miro1 expression in tauP301S transgenic mice ameliorates deficits in spatial learning and memory tests.

Using a contextual fear conditioning task,[84] we further examined the effects of Miro1 expression on contextual memory in mice at 7 months of age. TauP301S transgenic mice with or without AAV-Miro1 injection showed no significant difference from non-transgenic littermates on the training task before the foot shock (Fig. 8E). Non-transgenic mice injected with AAV-mCherry or AAV-mCherry-Miro1 exhibited contextual learning, with 41.77% and 45.34% of the time spent 'freezing' in the operant chamber in anticipation of the shock, respectively (Fig. 8E). However, tauP301S mice showed significant defects in this task, spending only 30.18% of the time freezing. Our data are consistent with previous studies,[44,45] suggesting defects in hippocampus-dependent memory in this tauopathy mouse model. Importantly, tauP301S mice expressing Miro1 exhibited significant amelioration of the learning deficit compared to tauP301S mice and performed similarly to non-transgenic mice. This result is in line with Miro1-mediated rescue effects on synaptic defects (Fig. 7 and Supplementary Fig. 7), suggesting that Miro1-enhanced healthy mitochondrial supply at tauopathy synapses is protective against the hippocampal-dependent memory impairment in tauP301S transgenic mice.

Synaptic plasticity has long been proposed to be a cellular mechanism underlying learning and memory. Given that we detected a significant improvement in the hippocampal-dependent behaviour in tauP301S transgenic mice with increasing Miro1 levels, we further performed long-term potentiation (LTP) recordings of the Schaffer collateral-CA1 pathway in the hippocampus from non-transgenic and tauP301S transgenic mice with and without overexpression of Miro1. Consistent with the results from previous studies,[44] the potentiation of the slope of field excitatory postsynaptic potentials (fEPSPs) induced by high-frequency stimulation is markedly reduced and remains low in tauP301S transgenic mice compared to non-transgenic mice injected with AAV-mCherry (Fig. 8F and G). However, elevated Miro1 expression significantly rescues the LTP defects in tauP301S mice. Collectively, these results demonstrate that overexpression of Miro1 exerts beneficial effects on synaptic plasticity and cognitive function in tauP301S transgenic mice.

Discussion

Neurodegeneration is thought to begin with the loss of presynaptic terminals and proceed retrogradely in a dying-back process. Synaptic stress occurs early in tauopathy brains and is associated with soluble pathogenic forms of tau in the absence of tau tangles, contributing to subsequent synapse loss and neurodegeneration.[41,44,46] Previous findings highlight a key role of soluble forms of phospho-tau in perturbing synaptic function.[7,64,85–88] Given that mitochondrial disturbances have been indicated at early disease stages of tauopathy, a fundamental question remains unanswered as to whether mitochondrial defects are involved in the early synaptic pathophysiology of tauopathy.

Our study uncovers, for the first time, an early mechanism by which activation of the Parkin pathway drives tauopathy-linked synaptic pathogenesis. We have revealed deficits in synaptic distribution of mitochondria in the brains of patients with tauopathies and two different tauopathy mouse models, which is associated with tauopathy well before axonal degeneration. Such a defect is caused by defective mitochondrial anterograde movement as a result of Parkin activation-induced excessive Miro1 degradation. Thus, the supply of mitochondria to tauopathy synapses is disrupted, impairing synaptic function. Furthermore, increasing Miro1 levels restores synaptic mitochondrial populations by enhancing anterograde transport of mitochondria, which protects against synaptic degeneration and cognitive impairment in tauopathy brains. It is important to note that mitochondrial retrograde transport is unaltered in tauopathy axons, excluding the possibility of the traffic jam resulting from tau aggregation or microtubule disassembly. We and others have demonstrated that retrograde transport facilitates removal of damaged mitochondria from synaptic terminals through Parkin-independent mechanisms for their clearance within lysosomes in the soma of neurons.[24,26,27,58,89–92] These findings allow us to propose that defects in mitochondrial

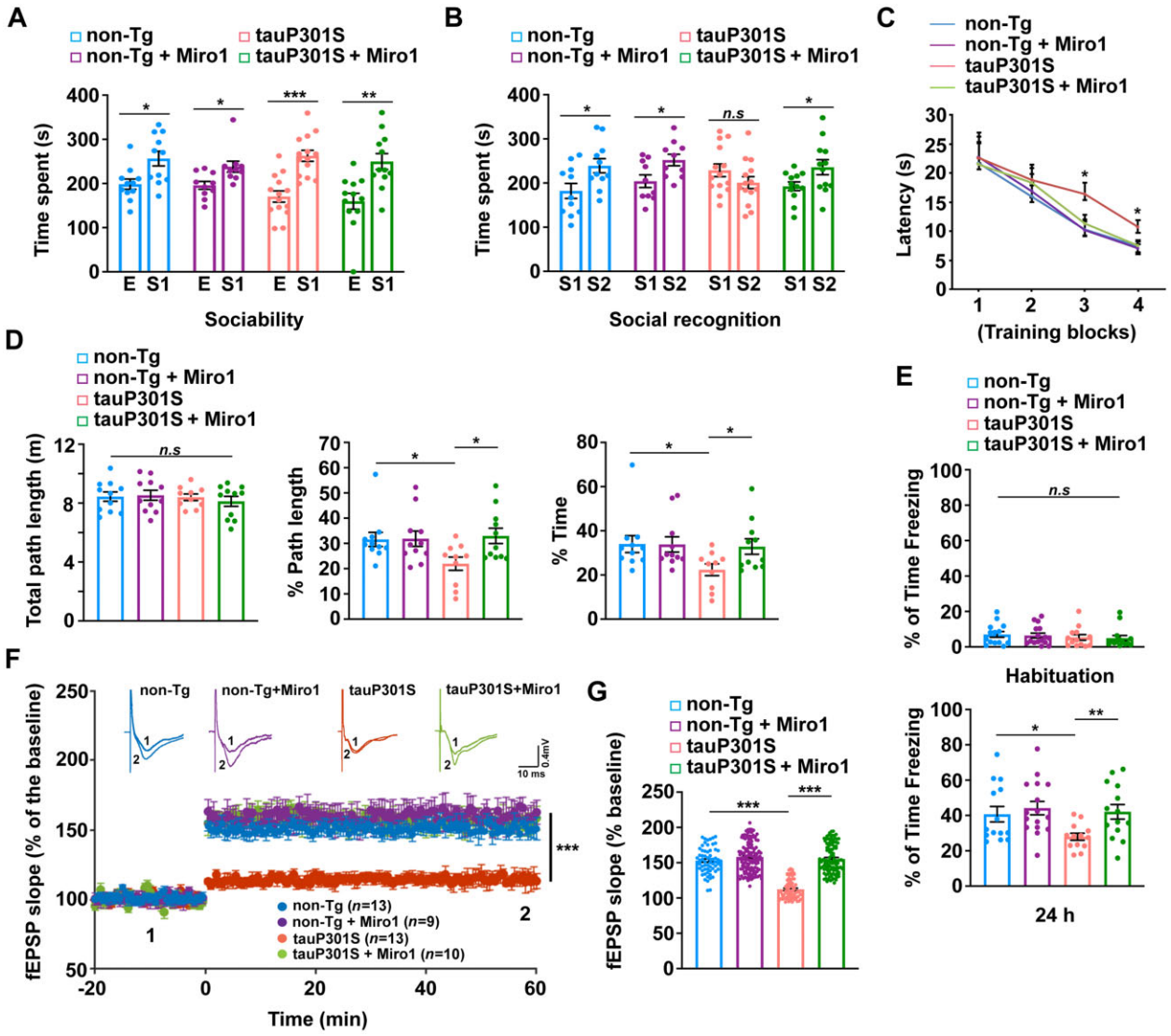

Figure 8 Elevated Miro1 expression improves behavioural performance and synaptic function in tau mice. (**A** and **B**) Elevated Miro1 expression ameliorates social recognition memory deficit in tauP301S transgenic mice (Tg) ($n = 10$–14 male mice; 6–7 months of age). Three-chamber tests were designed to measure both sociability (**A**) and social recognition memory (**B**). In the first session, sociability was measured with one chamber empty (E) and one chamber containing a stranger mouse (S1), whereas in the second session, social recognition memory was assessed with both chambers occupied: one housing the first, already-investigated familiar mouse (S1) and the other containing a novel stranger mouse (S2). In the first session, all four groups of mice spent longer time in the chamber with S1 over the empty chamber (E) [non-transgenic (non-Tg): $P < 0.05$; non-transgenic with Miro1: $P < 0.05$; tauP301S: $P < 0.001$; tauP301S with Miro1: $P < 0.01$; two-way ANOVA test] (**A**). In the second session, non-transgenic mice along with tauP301S transgenic mice injected with AAV-mCherry-Miro1 explored for longer in the chamber with S2 than in the familiar S1 chamber ($P < 0.05$; two-way ANOVA test) (**B**). Exploration time for tauP301S transgenic injected with AAV-mCherry control showed no significant difference in the chambers with the stranger mouse (S2) and the familiar mouse (S1) ($P > 0.05$; two-way ANOVA test). (**C** and **D**) Increasing Miro1 levels in tauP301S transgenic mouse brains prevents deficits in spatial learning and memory ($n = 10$–11 male mice per genotype; 7 months of age). Non-transgenic and tauP301S mice injected with AAV-mCherry control or AAV-mCherry-Miro1 were trained in the Morris water maze on a single day with four training blocks (three trials for block 1, which involved flagged platform training, and four trials each for blocks 2–4, which involved hidden-platform training). An interval of 3 min separated the initiation of each block. While time (latency) before reaching the platform was recorded, a probe trial (platform removed) was conducted 1 h after the last hidden-platform training. TauP301S transgenic mice show longer latency (time to find the hidden platform) than non-transgenic mice in training blocks 3 and 4 ($P < 0.05$; two-way ANOVA test) (**C**). Elevated Miro1 expression has no effect in non-transgenic mice at any given training block, but results in improved task learning in tauP301S mice ($P > 0.05$) (**C**). In the probe trial, tauP301S mice injected with AAV-mCherry, but not AAV-mCherry-Miro1, show less path length and less time in the target quadrant where the platform had previously been placed (**D**). Two-way ANOVA analysis of these data reveals a significant difference of tauP301S mice compared to non-transgenic mice ($P < 0.05$) and a rescue effect of AAV-mCherry-Miro1 injection in tauP301S transgenic mice ($P < 0.05$) but not in non-transgenic mice. No statistical significance is observed in total path length among all four groups of mice (**D**). (**E**) TauP301S transgenic mice injected with AAV-mCherry-Miro1 exhibit improvement in a hippocampus-dependent contextual fear conditioning task ($n = 13$–16 male mice; 7 months of age). All four groups show similar levels of freezing before the foot shock. However, tauP301S transgenic mice display reduced levels of freezing 24 h after the foot shock when compared to non-transgenic littermates ($P = 0.027$), which is attenuated by increasing Miro1 expression ($P = 0.008$; two-way ANOVA test). (**F** and **G**) Overexpression of Miro1 restores impaired LTP in tauP301S transgenic mouse brains at the age of 7–8 months. The slope of fEPSP in response to high-frequency stimulation (HFS: 100 Hz, three trains) delivered to the hippocampal Schaffer collateral-CA1 pathway from non-transgenic or tauP301S transgenic mice with or without overexpression of Miro1 (**F**). *Top*: Example fEPSP traces taken before (1) or after (2) stimulation. Calibration: 0.4 mV, 10 ms. n = number of slices per genotype. Quantification of average fEPSP slope in the last 10 min demonstrating impaired LTP in tauP301S transgenic mice and significant improvement after Miro1 elevation (**G**). Two-way ANOVA (between groups) followed by Tukey's HSD test. Error bars represent SEM. $^{***}P < 0.001$; $^{**}P < 0.01$; $^{*}P < 0.05$.

supply rather than abnormal retention of damaged mitochondria at tauopathy synapses are likely a key mechanism underlying early synaptic mitochondrial deficits and such a mechanism participates in the pathogenesis of synaptic failure associated with tauopathy.

Parkin-mediated mitophagy is initiated with Parkin translocation from the cytoplasm onto damaged mitochondria.[16,20–23] Using long time-lapse live cell imaging in mature cortical neurons, we have provided the first neuronal imaging evidence showing robust induction of Parkin-mediated mitophagy upon mitochondrial damage.[24,91] Several recent studies suggest a critical role of Parkin-mediated mitophagy in Alzheimer's disease pathophysiology.[35–40] In the current study, we have demonstrated that Parkin-mediated mitophagy is extensively activated in early tauopathy. Miro1 is a known target of proteasomal degradation upon Parkin activation.[28–32] Recent work from the Harper group has provided further information on the dynamics and specificity of Parkin-dependent ubiquitinylation in neurons. In the course of Parkin-mediated mitophagy, the degradation of Miro1 occurs early and is dispensable of Parkin-dependent subsequent ubiquitylation of a variety of mitochondrial outer membrane proteins.[55] In line with this work and our previous studies in normal neurons,[24,27,55] tauopathy neurons with 24-h CCCP treatment exhibited a reduction in Miro1 levels with no detectable changes of other mitochondrial proteins (Fig. 4C–E), indicating that Parkin activation-enhanced Miro1 turnover precedes mitophagy under tauopathy conditions. Moreover, loss of Parkin, but not OPTN or NDP52, rescues defects in mitochondrial anterograde transport and distribution in the axons and at the synapses of tauopathy neurons (Fig. 4H and I and Supplementary Figs 4E, F, 5A and B). This result suggests that blocking Parkin but not mitophagy downstream of Parkin activation reverses such defects. Combined with the biochemical evidence showing Miro1 reduction in tauopathy brains (Fig. 3E–H), we propose that excessive Miro1 degradation upon Parkin activation leads to defective mitochondrial anterograde movement towards tauopathy synapses. Importantly, increasing Miro1 levels enhances mitochondrial anterograde transport and protects against tauopathy-associated synaptic damage by restoring the synaptic supply of mitochondrial pools. Therefore, our study provides the first indication that extensive activation of the Parkin pathway triggers synaptic mitochondrial deficits, serving as an important mechanism underlying synaptic damage in stricken tauopathy neurons (Supplementary Fig. 9).

Pathogenic tau-induced mitochondrial transport and distribution impairment has been described in multiple systems, but the underlying mechanisms remain unclear. In a *Caenorhabditis elegans* model expressing highly amyloidogenic tau species, mitochondrial transport was perturbed by tau aggregation.[93] Changes in mitochondrial transport were also detected in tauopathy mouse brains,[94] accompanied by a reduced number of axonal mitochondria in cortical neurons derived from this model.[47] Altered mitochondrial distribution was reported in Alzheimer's disease patient brains with tauopathies,[19] which was correlated with the presence of soluble, but not aggregated tau. While our current study is in accord with these previous findings from the mammalian systems, we have further shown that mitochondrial anterograde movement is selectively impaired in axons associated with soluble phospho-tau accumulation. More importantly, defective anterograde transport of mitochondria in tauopathy axons is attributed to Parkin activation-enhanced Miro1 turnover that can be reversed by increasing Miro1 levels or blocking Parkin (Fig. 4A, B, H and I). Our current work is in accord with recent studies showing the involvement of increased mitophagy-linked excessive mitochondrial fragmentation and microtubule-dependent perinuclear clustering of mitochondria in mitochondrial optic neuropathies.[95,96] Thus, besides the previously proposed models,[19,47,94] our study has uncovered a new mechanism underlying phospho-tau-linked mitochondrial transport defects at the early disease stages, relevant to the development of synaptic degeneration associated with tauopathy.

Neuron-specific loss of Miro1 causes defects in Miro1-directed mitochondrial movement, depletion of mitochondria from axons and neurodegeneration in *Drosophila* and mouse models.[97,98] Recent studies reported Miro1 deficiency in neurons expressing amyotrophic lateral sclerosis-associated mutant SOD1, in the spinal cord tissues of amyotrophic lateral sclerosis patients and mouse models expressing SOD1 G93A or TDP-43 M337V.[99–101] Amyotrophic lateral sclerosis mutant SOD1 expression was shown to decrease Miro1 levels.[100] Interestingly, genetic ablation of Parkin attenuates the reduction in Miro1 levels and slows down motor neuron loss and muscle denervation in a mutant SOD1 mouse model,[101] suggesting the involvement of the Parkin pathway in amyotrophic lateral sclerosis-linked pathologies. In the current study, we have provided direct evidence showing decreases in Miro1 levels in the brains of FTD patients, Alzheimer's disease patients with tauopathies and mouse models. Furthermore, we have demonstrated that such a defect is linked to early tauopathy, resulting from accelerated Miro1 turnover upon broad activation of the Parkin pathway. Miro1 deficiency halts mitochondrial anterograde movement and hence induces deficits in the synaptic distribution of mitochondria, serving as an early mechanism underlying synaptic failure in tauopathy. In line with our new findings, we have further revealed that increasing Miro1 levels restores synaptic mitochondrial populations by reversing mitochondrial anterograde transport defects, thereby protecting against synaptic failure and cognitive deficits in tauopathy mouse models. Thus, our current study supports the premise that, as an effect of excessive Parkin activation, Miro1 deficiency is likely a general defect behind major neurodegenerative diseases associated with extensive mitochondrial stress, and further sheds light on a key mechanism underlying the pathogenesis of early tauopathy-linked synaptic dysfunction.

In summary, our work advances current knowledge of mitophagy regulation in tauopathy neurons and provides new insights into how extensive mitophagy activation induces synaptic mitochondrial deficiency and exacerbates synaptic damage in early tauopathy. The study opens new avenues for specifically targeting early synaptic dysfunction in tauopathies, and may have broader relevance to other neurodegenerative diseases associated with mitochondrial defects, altered mitochondrial quality control and impaired axonal transport.

Acknowledgements

We are grateful to D. Ganesan, E. Gavin, X. Su, Y. Parekh, P. Tiwari, H. Kaur and other members of the Cai Laboratory for technical assistance and constructive discussion; Y. Zuo and J. Yoon for critical reading; Z-H. Sheng for Myc-Miro1 plasmid; H. Imamura for AT1.03 plasmid; K. Ashe for GFP-tauP301L, GFP-AP/tauP301L and GFP-tau plasmids; D. Chan for pFUChW Parkin shRNA and pFUChW non-targeting shRNA; P. Davies for PHF1 antibody; W. Springer for pS65-Ub antibody; B. Albensi at University of Manitoba, S. Cheng at NINDS EM facility and R. Patel at EM facility in the Department of Pathology and Laboratory Medicine, Robert Wood Johnson Medical School for technical help; W-D. Yao, G-J. Xiong, Z. Pang and J-Y. Wu for technical help with electrophysiological recordings in cultured primary neurons and mouse brain slices; Harvard Tissue Resource Center supported by NIH Neurobiobank, National Institutes of Health grant HHSN-271–2013-00030C and Human Brain and Spinal Fluid Resource Center at UCLA for providing the

post-mortem brain specimens from Alzheimer's disease and FTD patients and age-matched control subjects.

Funding

This research was supported by National Institutes of Health grants R01NS089737, R01GM135326, and R21NS102780 (to Q.C.), R21HD091512 and R01NS102382 (to P.J.), R01DC015000 (to K.K.), R01NS089737 and NSF IOS-1845355 (to D.J.M.) and the Busch Biomedical Grant program and the Brain Health Institute, Rutgers University (to A.K.).

Competing interests

The authors report no competing interests.

Supplementary material

Supplementary material is available at *Brain* online.

References

1. Fukui H, Moraes CT. The mitochondrial impairment, oxidative stress and neurodegeneration connection: Reality or just an attractive hypothesis? *Trends Neurosci*. 2008;31(5):251–256.
2. Swerdlow RH, Burns JM, Khan SM. The Alzheimer's disease mitochondrial cascade hypothesis. *J Alzheimers Dis*. 2010; 20(Suppl 2):S265–S279.
3. Reddy PH, Beal MF. Amyloid beta, mitochondrial dysfunction and synaptic damage: Implications for cognitive decline in aging and Alzheimer's disease. *Trends Mol Med*. 2008;14(2): 45–53.
4. Gendron TF, Petrucelli L. The role of tau in neurodegeneration. *Mol Neurodegener*. 2009;4:13.
5. Mandelkow EM, Mandelkow E. Biochemistry and cell biology of tau protein in neurofibrillary degeneration. *Cold Spring Harb Perspect Med*. 2012;2(7):a006247.
6. Giannakopoulos P, Herrmann FR, Bussiere T, et al. Tangle and neuron numbers, but not amyloid load, predict cognitive status in Alzheimer's disease. *Neurology*. 2003;60(9):1495–1500.
7. Santacruz K, Lewis J, Spires T, et al. Tau suppression in a neurodegenerative mouse model improves memory function. *Science*. 2005;309(5733):476–481.
8. Ramsden M, Kotilinek L, Forster C, et al. Age-dependent neurofibrillary tangle formation, neuron loss, and memory impairment in a mouse model of human tauopathy (P301L). *J Neurosci*. 2005;25(46):10637–10647.
9. Reddy PH. Abnormal tau, mitochondrial dysfunction, impaired axonal transport of mitochondria, and synaptic deprivation in Alzheimer's disease. *Brain Res*. 2011;1415:136–148.
10. Eckert A, Nisbet R, Grimm A, Gotz J. March separate, strike together—Role of phosphorylated TAU in mitochondrial dysfunction in Alzheimer's disease. *Biochim Biophys Acta*. 2014; 1842(8):1258–1266.
11. Spires-Jones TL, Hyman BT. The intersection of amyloid beta and tau at synapses in Alzheimer's disease. *Neuron*. 2014;82(4): 756–771.
12. Cai Q, Tammineni P. Alterations in mitochondrial quality control in Alzheimer's disease. *Front Cell Neurosci*. 2016;10:24.
13. Reddy PH, Oliver DM. Amyloid beta and phosphorylated tau-induced defective autophagy and mitophagy in Alzheimer's disease. *Cells*. 2019;8(5):488.
14. Manczak M, Reddy PH. Abnormal interaction of VDAC1 with amyloid beta and phosphorylated tau causes mitochondrial dysfunction in Alzheimer's disease. *Hum Mol Genet*. 2012; 21(23):5131–5146.
15. Cai Q, Tammineni P. Mitochondrial aspects of synaptic dysfunction in Alzheimer's disease. *J Alzheimers Dis*. 2017;57(4): 1087–1103.
16. Cai Q, Jeong YY. Mitophagy in Alzheimer's disease and other age-related neurodegenerative diseases. *Cells*. 2020;9(1):150.
17. Dumont M, Stack C, Elipenahli C, et al. Behavioral deficit, oxidative stress, and mitochondrial dysfunction precede tau pathology in P301S transgenic mice. *FASEB J*. 2011;25(11): 4063–4072.
18. Lopez-Gonzalez I, Aso E, Carmona M, et al. Neuroinflammatory gene regulation, mitochondrial function, oxidative stress, and brain lipid modifications with disease progression in tau P301S transgenic mice as a model of frontotemporal lobar degeneration-tau. *J Neuropathol Exp Neurol*. 2015;74(10):975–999.
19. Kopeikina KJ, Carlson GA, Pitstick R, et al. Tau accumulation causes mitochondrial distribution deficits in neurons in a mouse model of tauopathy and in human Alzheimer's disease brain. *Am J Pathol*. 2011;179(4):2071–2082.
20. Youle RJ, Narendra DP. Mechanisms of mitophagy. *Nat Rev Mol Cell Biol*. 2011;12(1):9–14.
21. Sheng ZH, Cai Q. Mitochondrial transport in neurons: Impact on synaptic homeostasis and neurodegeneration. *Nat Rev Neurosci*. 2012;13(2):77–93.
22. Pickles S, Vigie P, Youle RJ. Mitophagy and quality control mechanisms in mitochondrial maintenance. *Curr Biol*. 2018; 28(4):R170–R185.
23. Pickrell AM, Youle RJ. The roles of PINK1, Parkin, and mitochondrial fidelity in Parkinson's disease. *Neuron*. 2015;85(2): 257–273.
24. Cai Q, Zakaria HM, Simone A, Sheng ZH. Spatial Parkin translocation and degradation of damaged mitochondria via mitophagy in live cortical neurons. *Curr Biol*. 2012;22(6): 545–552.
25. Sung H, Tandarich LC, Nguyen K, Hollenbeck PJ. Compartmentalized regulation of Parkin-mediated mitochondrial quality control in the drosophila nervous system *in vivo*. *J Neurosci*. 2016;36(28):7375–7391.
26. Devireddy S, Liu A, Lampe T, Hollenbeck PJ. The organization of mitochondrial quality control and life cycle in the nervous system *in vivo* in the absence of PINK1. *J Neurosci*. 2015;35(25): 9391–9401.
27. Lin MY, Cheng XT, Tammineni P, et al. Releasing syntaphilin removes stressed mitochondria from axons independent of mitophagy under pathophysiological conditions. *Neuron*. 2017; 94(3):595–610.e6.
28. Bingol B, Tea JS, Phu L, et al. The mitochondrial deubiquitinase USP30 opposes Parkin-mediated mitophagy. *Nature*. 2014; 510(7505):370–375.
29. Birsa N, Norkett R, Wauer T, et al. Lysine 27 ubiquitination of the mitochondrial transport protein Miro is dependent on serine 65 of the Parkin ubiquitin ligase. *J Biol Chem*. 2014;289(21): 14569–14582.
30. Chan NC, Salazar AM, Pham AH, et al. Broad activation of the ubiquitin–proteasome system by Parkin is critical for mitophagy. *Hum Mol Genet*. 2011;20(9):1726–1737.
31. Liu S, Sawada T, Lee S, et al. Parkinson's disease-associated kinase PINK1 regulates Miro protein level and axonal transport of mitochondria. *PLoS Genet*. 2012;8(3):e1002537.
32. Wang X, Winter D, Ashrafi G, et al. PINK1 and Parkin target Miro for phosphorylation and degradation to arrest mitochondrial motility. *Cell*. 2011;147(4):893–906.

33. Moreira PI, Siedlak SL, Wang X, et al. Autophagocytosis of mitochondria is prominent in Alzheimer disease. *J Neuropathol Exp Neurol*. 2007;66(6):525–532.
34. Moreira PI, Siedlak SL, Wang X, et al. Increased autophagic degradation of mitochondria in Alzheimer disease. *Autophagy*. 2007;3(6):614–615.
35. Ye X, Sun X, Starovoytov V, Cai Q. Parkin-mediated mitophagy in mutant hAPP neurons and Alzheimer's disease patient brains. *Hum Mol Genet*. 2015;24(10):2938–2951.
36. Du F, Yu Q, Yan S, et al. PINK1 signalling rescues amyloid pathology and mitochondrial dysfunction in Alzheimer's disease. *Brain*. 2017;140(12):3233–3251.
37. Manczak M, Kandimalla R, Yin X, Reddy PH. Hippocampal mutant APP and amyloid beta-induced cognitive decline, dendritic spine loss, defective autophagy, mitophagy and mitochondrial abnormalities in a mouse model of Alzheimer's disease. *Hum Mol Genet*. 2018;27(8):1332–1342.
38. Reddy PH, Yin X, Manczak M, et al. Mutant APP and amyloid beta-induced defective autophagy, mitophagy, mitochondrial structural and functional changes and synaptic damage in hippocampal neurons from Alzheimer's disease. *Hum Mol Genet*. 2018;27(14):2502–2516.
39. Cummins N, Tweedie A, Zuryn S, Bertran-Gonzalez J, Gotz J. Disease-associated tau impairs mitophagy by inhibiting Parkin translocation to mitochondria. *EMBO J*. 2019;38(3): e99360.
40. Fang EF, Hou Y, Palikaras K, et al. Mitophagy inhibits amyloid-beta and tau pathology and reverses cognitive deficits in models of Alzheimer's disease. *Nat Neurosci*. 2019;22(3):401–412.
41. Yoshiyama Y, Higuchi M, Zhang B, et al. Synapse loss and microglial activation precede tangles in a P301S tauopathy mouse model. *Neuron*. 2007;53(3):337–351.
42. Franklin KBJ, Paxinos G. The mouse brain in stereotaxic coordinates, 2nd edition. San Diego: Academic Press. 2001.
43. Ye X, Feng T, Tammineni P, et al. Regulation of synaptic amyloid-beta generation through BACE1 retrograde transport in a mouse model of Alzheimer's disease. *J Neurosci*. 2017;37(10): 2639–2655.
44. Litvinchuk A, Wan YW, Swartzlander DB, et al. Complement C3aR inactivation attenuates tau pathology and reverses an immune network deregulated in tauopathy models and Alzheimer's disease. *Neuron*. 2018;100(6):1337–1353.e5.
45. Takeuchi H, Iba M, Inoue H, et al. P301S mutant human tau transgenic mice manifest early symptoms of human tauopathies with dementia and altered sensorimotor gating. *PLoS One*. 2011;6(6):e21050.
46. Koss DJ, Jones G, Cranston A, Gardner H, Kanaan NM, Platt B. Soluble pre-fibrillar tau and beta-amyloid species emerge in early human Alzheimer's disease and track disease progression and cognitive decline. *Acta Neuropathol*. 2016;132(6): 875–895.
47. Rodriguez-Martin T, Pooler AM, Lau DHW, et al. Reduced number of axonal mitochondria and tau hypophosphorylation in mouse P301L tau knockin neurons. *Neurobiol Dis*. 2016;85:1–10.
48. Spires TL, Orne JD, SantaCruz K, et al. Region-specific dissociation of neuronal loss and neurofibrillary pathology in a mouse model of tauopathy. *Am J Pathol*. 2006;168(5):1598–1607.
49. Waypa GB, Marks JD, Guzy R, et al. Hypoxia triggers subcellular compartmental redox signaling in vascular smooth muscle cells. *Circ Res*. 2010;106(3):526–535.
50. Xie H, Guan J, Borrelli LA, Xu J, Serrano-Pozo A, Bacskai BJ. Mitochondrial alterations near amyloid plaques in an Alzheimer's disease mouse model. *J Neurosci*. 2013;33(43): 17042–17051.
51. Imamura H, Nhat KP, Togawa H, et al. Visualization of ATP levels inside single living cells with fluorescence resonance energy transfer-based genetically encoded indicators. *Proc Natl Acad Sci U S A*. 2009;106(37):15651–15656.
52. Kane LA, Lazarou M, Fogel AI, et al. PINK1 phosphorylates ubiquitin to activate Parkin E3 ubiquitin ligase activity. *J Cell Biol*. 2014;205(2):143–153.
53. Koyano F, Okatsu K, Kosako H, et al. Ubiquitin is phosphorylated by PINK1 to activate Parkin. *Nature*. 2014;510(7503): 162–166.
54. Fiesel FC, Ando M, Hudec R, et al. (Patho-)physiological relevance of PINK1-dependent ubiquitin phosphorylation. *EMBO Rep*. 2015;16(9):1114–1130.
55. Ordureau A, Paulo JA, Zhang J, et al. Global landscape and dynamics of Parkin and USP30-dependent ubiquitylomes in iNeurons during mitophagic signaling. *Mol Cell*. 2020;77(5): 1124–1142.e10.
56. Klionsky DJ, Abdel-Aziz AK, Abdelfatah S, et al. Guidelines for the use and interpretation of assays for monitoring autophagy (4th edition). *Autophagy*. 2021;17(1):1–382.
57. Manczak M, Reddy PH. Abnormal interaction between the mitochondrial fission protein Drp1 and hyperphosphorylated tau in Alzheimer's disease neurons: Implications for mitochondrial dysfunction and neuronal damage. *Hum Mol Genet*. 2012;21(11):2538–2547.
58. Han S, Jeong YY, Sheshadri P, Su X, Cai Q. Mitophagy regulates integrity of mitochondria at synapses and is critical for synaptic maintenance. *EMBO Rep*. 2020;21(9):e201949801.
59. Rojansky R, Cha MY, Chan DC. Elimination of paternal mitochondria in mouse embryos occurs through autophagic degradation dependent on PARKIN and MUL1. *Elife*. 2016;5:e17896.
60. Lazarou M, Sliter DA, Kane LA, et al. The ubiquitin kinase PINK1 recruits autophagy receptors to induce mitophagy. *Nature*. 2015;524(7565):309–314.
61. Moore AS, Holzbaur EL. Dynamic recruitment and activation of ALS-associated TBK1 with its target optineurin are required for efficient mitophagy. *Proc Natl Acad Sci U S A*. 2016;113(24): E3349–E3358.
62. Wong YC, Holzbaur EL. Optineurin is an autophagy receptor for damaged mitochondria in Parkin-mediated mitophagy that is disrupted by an ALS-linked mutation. *Proc Natl Acad Sci U S A*. 2014;111(42):E4439–E4448.
63. Heo JM, Ordureau A, Paulo JA, Rinehart J, Harper JW. The PINK1-PARKIN mitochondrial ubiquitylation pathway drives a program of OPTN/NDP52 recruitment and TBK1 activation to promote mitophagy. *Mol Cell*. 2015;60(1):7–20.
64. Hoover BR, Reed MN, Su J, et al. Tau mislocalization to dendritic spines mediates synaptic dysfunction independently of neurodegeneration. *Neuron*. 2010;68(6):1067–1081.
65. Pan PY, Cai Q, Lin L, Lu PH, Duan S, Sheng ZH. SNAP-29-mediated modulation of synaptic transmission in cultured hippocampal neurons. *J Biol Chem*. 2005;280(27):25769–25779.
66. Cai Q, Gerwin C, Sheng ZH. Syntabulin-mediated anterograde transport of mitochondria along neuronal processes. *J Cell Biol*. 2005;170(6):959–969.
67. Kang JS, Tian JH, Pan PY, et al. Docking of axonal mitochondria by syntaphilin controls their mobility and affects short-term facilitation. *Cell*. 2008;132(1):137–148.
68. Cai Q, Lu L, Tian JH, Zhu YB, Qiao H, Sheng ZH. Snapin-regulated late endosomal transport is critical for efficient autophagy-lysosomal function in neurons. *Neuron*. 2010;68(1):73–86.
69. Nagahara AH, Mateling M, Kovacs I, et al. Early BDNF treatment ameliorates cell loss in the entorhinal cortex of APP transgenic mice. *J Neurosci*. 2013;33(39):15596–15602.

70. Polito VA, Li H, Martini-Stoica H, et al. Selective clearance of aberrant tau proteins and rescue of neurotoxicity by transcription factor EB. *EMBO Mol Med*. 2014;6(9):1142–1160.
71. Nagahara AH, Merrill DA, Coppola G, et al. Neuroprotective effects of brain-derived neurotrophic factor in rodent and primate models of Alzheimer's disease. *Nat Med*. 2009;15(3):331–337.
72. Xiao Q, Yan P, Ma X, et al. Neuronal-targeted TFEB accelerates lysosomal degradation of APP, reducing abeta generation and amyloid plaque pathogenesis. *J Neurosci*. 2015;35(35):12137–12151.
73. Xie Y, Zhou B, Lin MY, Wang S, Foust KD, Sheng ZH. Endolysosomal deficits augment mitochondria pathology in spinal motor neurons of asymptomatic fALS mice. *Neuron*. 2015;87(2):355–370.
74. Davis AF, Clayton DA. In situ localization of mitochondrial DNA replication in intact mammalian cells. *J Cell Biol*. 1996;135(4):883–893.
75. Taniguchi T, Doe N, Matsuyama S, et al. Transgenic mice expressing mutant (N279K) human tau show mutation dependent cognitive deficits without neurofibrillary tangle formation. *FEBS Lett*. 2005;579(25):5704–5712.
76. Scattoni ML, Gasparini L, Alleva E, Goedert M, Calamandrei G, Spillantini MG. Early behavioural markers of disease in P301S tau transgenic mice. *Behav Brain Res*. 2010;208(1):250–257.
77. Trantham-Davidson H, Vazdarjanova A, Dai R, Terry A, Bergson C. Up-regulation of calcyon results in locomotor hyperactivity and reduced anxiety in mice. *Behav Brain Res*. 2008;189(2):244–249.
78. Suemaru S, Hashimoto K, Suemaru K, Maeba Y, Matsushita N, Ota Z. Hyperkinesia, plasma corticotropin releasing hormone and ACTH in senile dementia. *Neuroreport*. 1991;2(6):337–340.
79. Crawley JN. Designing mouse behavioral tasks relevant to autistic-like behaviors. *Ment Retard Dev Disabil Res Rev*. 2004;10(4):248–258.
80. Moy SS, Nadler JJ, Perez A, et al. Sociability and preference for social novelty in five inbred strains: An approach to assess autistic-like behavior in mice. *Genes Brain Behav*. 2004;3(5):287–302.
81. Nadler JJ, Moy SS, Dold G, et al. Automated apparatus for quantitation of social approach behaviors in mice. *Genes Brain Behav*. 2004;3(5):303–314.
82. Nunez J. Morris water maze experiment. *J Vis Exp*. 2008;(19):897.
83. Glass R, Norton S, Fox N, Kusnecov AW. Maternal immune activation with staphylococcal enterotoxin A produces unique behavioral changes in C57BL/6 mouse offspring. *Brain Behav Immun*. 2019;75:12–25.
84. Phillips RG, LeDoux JE. Differential contribution of amygdala and hippocampus to cued and contextual fear conditioning. *Behav Neurosci*. 1992;106(2):274–285.
85. Rocher AB, Crimins JL, Amatrudo JM, et al. Structural and functional changes in tau mutant mice neurons are not linked to the presence of NFTs. *Exp Neurol*. 2010;223(2):385–393.
86. Crimins JL, Rocher AB, Luebke JI. Electrophysiological changes precede morphological changes to frontal cortical pyramidal neurons in the rTg4510 mouse model of progressive tauopathy. *Acta Neuropathol*. 2012;124(6):777–795.
87. Polydoro M, Dzhala VI, Pooler AM, et al. Soluble pathological tau in the entorhinal cortex leads to presynaptic deficits in an early Alzheimer's disease model. *Acta Neuropathol*. 2014;127(2):257–270.
88. McInnes J, Wierda K, Snellinx A, et al. Synaptogyrin-3 mediates presynaptic dysfunction induced by tau. *Neuron*. 2018;97(4):823–835.e8.
89. Miller KE, Sheetz MP. Axonal mitochondrial transport and potential are correlated. *J Cell Sci*. 2004;117(Pt 13):2791–2804.
90. Han S, Jeong YY, Sheshadri P, Cai Q. Mitophagy coordination with retrograde transport ensures the integrity of synaptic mitochondria. *Autophagy*. 2020;16(10):1925–1927.
91. Cai Q, Zakaria HM, Sheng ZH. Long time-lapse imaging reveals unique features of PARK2/Parkin-mediated mitophagy in mature cortical neurons. *Autophagy*. 2012;8(6):976–978.
92. Lin MY, Cheng XT, Xie Y, Cai Q, Sheng ZH. Removing dysfunctional mitochondria from axons independent of mitophagy under pathophysiological conditions. *Autophagy*. 2017;13(10):1792–1793.
93. Fatouros C, Pir GJ, Biernat J, et al. Inhibition of tau aggregation in a novel *Caenorhabditis elegans* model of tauopathy mitigates proteotoxicity. *Hum Mol Genet*. 2012;21(16):3587–3603.
94. Gilley J, Seereeram A, Ando K, et al. Age-dependent axonal transport and locomotor changes and tau hypophosphorylation in a 'P301L' tau knockin mouse. *Neurobiol Aging*. 2012;33(3):621.e1–621.e15.
95. Liao C, Ashley N, Diot A, et al. Dysregulated mitophagy and mitochondrial organization in optic atrophy due to *OPA1* mutations. *Neurology*. 2017;88(2):131–142.
96. Dombi E, Diot A, Morten K, et al. The m.13051G>A mitochondrial DNA mutation results in variable neurology and activated mitophagy. *Neurology*. 2016;86(20):1921–1923.
97. Iijima-Ando K, Sekiya M, Maruko-Otake A, et al. Loss of axonal mitochondria promotes tau-mediated neurodegeneration and Alzheimer's disease-related tau phosphorylation via PAR-1. *PLoS Genet*. 2012;8(8):e1002918.
98. Nguyen TT, Oh SS, Weaver D, et al. Loss of Miro1-directed mitochondrial movement results in a novel murine model for neuron disease. *Proc Natl Acad Sci U S A*. 2014;111(35):E3631–E3640.
99. Zhang F, Wang W, Siedlak SL, et al. Miro1 deficiency in amyotrophic lateral sclerosis. *Front Aging Neurosci*. 2015;7:100.
100. Moller A, Bauer CS, Cohen RN, Webster CP, De Vos KJ. Amyotrophic lateral sclerosis-associated mutant SOD1 inhibits anterograde axonal transport of mitochondria by reducing Miro1 levels. *Hum Mol Genet*. 2017;26(23):4668–4679.
101. Palomo GM, Granatiero V, Kawamata H, et al. Parkin is a disease modifier in the mutant SOD1 mouse model of ALS. *EMBO Mol Med*. 2018;10(10):e8888.